Heinz Gerischer, March 31st, 1919, Wittenberg till September 14th, 1994, Berlin
and
Wolf Vielstich, June 18th, 1923, Munich till August 27th, 2021, Bonn

Article

Zeitschrift für Physikalische Chemie, New Series, Vol. 3 and 4, pp. 16–33 and pp. 10–23 (1955)

Contents

I. On electrolysis at constant electrode potential. I. The time-current curve with inhibited discharge with subsequent delivery through diffusion and conclusions about the kinetics 4

1. Abstract 6

2. Problem Statement 7

3. Derivation of the Current Curve over Time 10
- 3.1. General Description 10
- 3.2. I. Simplified Reaction Types 11
- 3.3. II. General Case – ”Discharge with Diffusion in both Phases” 12
- 3.4. The Involvement of Fast, Upstream Reactions 15

4. Discussion and Conclusions about the Reaction Mechanism 17
- 4.1. Determination of the ”Initial Potential-Current Curve” 17
- 4.2. Determination of the Exchange Current Density and the Charge Transfer Coefficient 19
- 4.3. Analysis of the Reaction Mechanism 19
- 4.4. Comparison With Other Methods 22

II. On electrolysis at constant potential. II. Studies on the kinetics of the deposition of simple zinc and complex silver ions 23

1. Abstract 25

2. Experimental Setup 26
- 2.1. The Potentiostat 26
- 2.2. The Measuring Cells 28
- 2.3. Preparation of the Solutions. Pretreatment of the Electrodes 29

3. Discharge of Simple Zn^{2+}-Ions on Zn-Amalgam **31**
3.1. Time-Current curve 31
3.2. Determination of Kinetic Data 34

4. Discharge of complex Ag^+ Ions **36**
4.1. Complexes with Cyanide 36
4.2. Ag^+ Complexes with Ammonia 38

III. Appendix **44**

1. Calculation of the concentration curve over time **45**

References **49**

Part I.

On electrolysis at constant electrode potential. I. The time-current curve with inhibited discharge with subsequent delivery through diffusion and conclusions about the kinetics

With 3 figures in text. (Received on 11.8.54.)

1. Abstract

The adjustment process on an electrode after applying a constant potential is examined. From the time-current curve, an ”initial current intensity” can be determined by extrapolation to the time of switching on. This is solely determined by the speed of the discharge process. Therefore, information about the kinetics of the discharge reaction can be obtained from this, which is explained in more detail for the discharge of simple and complex metal ions. Particularly for the latter case, the potentiostatic method provides a very simple way to analyze the reaction mechanism.

2. Problem Statement

When an electric current flows through an electrolytic cell, polarization voltages occur at the electrodes, which reduce the effective cell voltage. The cause of these polarization voltages are changes in the concentration of the substances involved in the discharge process, which cannot be provided quickly enough (so-called concentration or "delivery" polarization), and the energy threshold at the phase boundary, which must be overcome when the electrical charge carrier passes through (activation polarization).

If no special precautions are taken, once electrolysis begins, the current and voltage will always change simultaneously until a steady state is reached. The electrode polarization in the steady state is essentially determined by the slowest sub-process of the gross electrode reaction. These are often uncharacteristic transport processes. If one wants to find out something about the actual discharge reaction in such cases, one has to examine the adjustment processes during time.

The concentration distribution in front of the electrode with its complicated spatial and temporal progression cannot be directly determined experimentally. Only the electrode potential and electrolysis current can be measured. However, evaluating the adjustment process is very complicated when these two measured variables are changed at the same time. It is significantly simplified if the experimental conditions are chosen so that one of the two measured variables remains constant. Since this can be achieved particularly easily for the electrolysis current by choosing a power source with a very high voltage and connecting a correspondingly high-impedance resistor, this so-called "galvanostatic" method has been used very frequently[1], [20, 8]. However, the theoretical evaluation of such measurements of the time-potential curve presents a fundamental difficulty. As is well known, the phase boundary of the electrode also has the properties of a capacitor with a very large capacity. The directly measurable electrolysis current i is divided at the electrode into the charging current $C \cdot \frac{\mathrm{d}\varepsilon}{\mathrm{d}t}$ and the charge transfer current j. All kinetic equations between current, potential and concentration of the substances involved in the discharge process, which must be used to evaluate the measured polarization-time curves, refer to the charge transfer current. However, this cannot be measured directly. In the galvanostatic arrangement described above, the electrolysis current is kept constant. The desired simplification for the evaluation of the time-potential curve is therefore only achieved if the charging current is negligible. However, this is not the case for short-term processes.

---

[1] An overview of the older work can be found at [4].

With electrolysis with a constant electrode potential, the so-called potentiostatic process, this difficulty no longer applies, provided that the electrode capacity does not change over time despite the constant potential. The latter can always be kept negligibly small if the composition of the electrolyte is chosen in a definite manner, provided that coating layers do not form on the electrode during electrolysis. However, the experimental difficulties in realizing the potentiostatic condition are incomparably greater.

A potentiostatic circuit must meet two requirements. First, after switching on the current, the test electrode should be brought from its resting potential (ε_0 at $i = 0$) to the desired polarization potential ε in the shortest time possible, whereby the double-layer capacitor must be charged. The current must then always be regulated in such a way that this potential is maintained, i.e. the voltage source must be controlled in such a way that it just compensates for the inevitable ohmic voltage drop that occurs in the circuit as well as any polarization voltage at the counter electrode. Such arrangements have recently been implemented with sufficient quality using electronic control devices, [29]. This will be reported in the following experimental study when treating the potentiostat we used.

The time course of the current during such a potentiostatic voltage surge essentially depends on the subsequent delivery and removal processes for the substances reacting at the electrode. These are transport processes and upstream chemical reactions. The course of the time-current curve is determined by their speed, their relationship to one another and to the discharge reaction[2]. If one knows what time sequence is to be expected for certain types of reactions, one can draw conclusions about the reaction mechanism from the experimental curves and also determine the speed of the sub-processes.

In this work we want to derive the time course of the current for the important reaction type in which an inhibited discharge process is coupled with diffusion on both sides of the phase boundary as subsequent delivery processes. A formally similar calculation for the coupling of upstream reaction with diffusion without discharge inhibition was carried out by Delahay, [6], in connection with his studies on irreversible, polarographic waves. Furthermore, Smutek, [30], has given an exact solution to this problem in terms of polarography.

The course of the current when upstream chemical reactions are involved can be covered in such cases using our simpler calculation, provided that the reaction equilibrium is reached quickly compared to the discharge rate. A general treatment of the behavior of such systems will be provided in a future publication.

The speed of the sub-processes, in particular that of the discharge process, can be deduced from the current characteristic over time. What conclusions can be drawn from this regarding the reaction mechanism will be discussed specifically with regard to the analysis of the mechanism of the discharge of complex ions. Examples of the practical application of these relationships will be given in a subsequent communication.

---

[2] A particular advantage of the potentiostatic condition is that the exponential dependence of the discharge speed on the potential, which is extremely difficult to solve when the potential is variable, is without effect for the calculation of the differential equations governing the system.

3. Derivation of the Current Curve over Time

3.1. General Description

We consider an electrode on which the following discharge process shall take place:

$$\mathrm{M} \rightleftharpoons \mathrm{M}^{n+} + ne^{-} \tag{3.1}$$

and track the current after a definite overvoltage is switched on, i.e. at a certain deviation of the electrode potential from the equilibrium value. The subsequent delivery of the substances consumed at the electrode or the removal of the substances produced there should only take place through diffusion[1].
The electrode shall be flat and the boundary of the diffusion space is chosen such that the diffusion processes only take place perpendicular to the electrode surface and can be treated one-dimensionally.
A kinetic relationship applies to the electrode current density, which was first derived by BUTLER, [2, 3], and will be used here in the following form, [13]:

$$j = j_0 \cdot \left[\frac{c_r}{{}_0c_r} \cdot e^{\alpha \cdot \frac{n}{\Phi} \cdot \eta} - \frac{c_{0x}}{{}_0c_{0x}} \cdot e^{-(1-\alpha) \cdot \frac{n}{\Phi} \cdot \eta} \right] \tag{3.2}$$

j_0 = exchange current density at equilibrium potential

$$j_0 = {}_0c_r^{(1-\alpha)} \cdot {}_0c_{0x}^{\alpha} \cdot {}^0j \tag{3.2a}$$

---

[1] We therefore assume that convection and transport through electrical transfer are excluded, the latter through a sufficient excess of foreign electrolyte.

α = charge transfer coefficient ($0 < \alpha < 1$)
η = $\varepsilon - \varepsilon_0$ = Overvoltage
ε_0 = equilibrium potential, measured against a reference electrode
Φ = $\frac{\mathscr{R}T}{\mathscr{F}}$
n = number of electrons involved in the electrode reaction, change of valency at electrode reaction.
c_r = Concentration of the reducing, discharge-determining component at the phase boundary (in the case of Equation 3.1 e.g. M)
c_{0x} = Concentration of the oxidizing, discharge-determining component at the phase boundary (e.g. $\left[\mathrm{M}^{n+}\right]$ in Equation 3.1)
${}_0c_r$ und ${}_0c_{0x}$ = corresponding concentrations in the initial state (equilibrium).

In the ideal case of a potentiostatic switch-on process, the constant overvoltage is set immediately at time $t = 0$. Accordingly, a definite charge transfer current flows immediately. While c_r and c_{0x} had their equilibrium values ${}_0c_r$ and ${}_0c_{0x}$ at the phase boundary until the overvoltage was switched on, concentration changes now occur immediately due to the substance conversion associated with the current flow. c_r and c_{0x} become functions of time ($c_r(t)$ and $c_{0x}(t)$) and in turn determine the time course of the charge transfer current according to Equation 3.2. Therefore, calculating the time course of the concentrations $c_r(t)$ and $c_{0x}(t)$ immediately results in the current j also.
Assuming that only diffusion is decisive for the transport processes on both sides of the phase boundary, we can easily formulate the mathematical problem that has to be solved to calculate the time course of the concentration using the differential equation for diffusion with the corresponding boundary conditions. Before we explain this, let us briefly mention a few special cases of this problem, the solutions to which have long been known.

3.2. I. Simplified Reaction Types

The first trivial case is where the discharge is inhibited to a large extend and the diffusion by contrast occurs quickly[2]. Then the concentrations at the phase boundary remain almost constant and one finds:

$$j = \text{const.} = j_0 \cdot \left(e^{\alpha \cdot \frac{n}{\Phi} \cdot \eta} - e^{-(1-\alpha) \cdot \frac{n}{\Phi} \cdot \eta}\right) = I_a^+(\eta) - I_a^-(\eta) = I_a(\eta)\,. \qquad (3.3)$$

---

[2] For example, if the transport velocity is high due to strong convection, which is easier to achieve.

The case has long been known in which the discharge rate is very high compared to the delivery rate and concentration polarization only occurs in one phase (e.g. when Hg^+ is deposited on Hg) or at least remains negligible in one phase (e.g. when ${}_0c_r \gg {}_0c_{0x}$ or vice versa). This is the case of the so-called "absolute concentration polarization"[3], in which it is assumed that the concentration at the phase boundary is set, according to the Nernst relationship, to the equilibrium value almost immediately after the voltage is switched on: (assuming $c_r(t) = {}_0c_r = \text{const.}$):

$$\frac{c_{0x}}{{}_0c_{0x}} = e^{\frac{n}{\Phi}\cdot\eta}\,. \tag{3.4}$$

Here the transport process is the sole determining factor for the current. One gets, [5, 23]:

$$j = \frac{L}{\sqrt{t}} \quad \text{with} \quad L = n\cdot\mathscr{F}\cdot{}_0c_{0x}\cdot\sqrt{\frac{\mathscr{D}}{\pi}}\cdot\left(e^{\frac{n}{\Phi}\cdot\eta}-1\right)\,. \tag{3.5}$$

This relationship has been confirmed experimentally many times and was used to determine the diffusion coefficient, [26, 31]. The fact that Equation 3.5 cannot correctly reproduce the time-current curve over the entire range can be seen from the limiting case $t \to 0$, where the physically impossible conclusion $j \to \infty$ would result. The assumption of this calculation cannot apply to very short periods of time. The current there is not determined by the subsequent delivery process, but by the discharge speed as the slowest sub-process. This statement generally applies, regardless of the type of subsequent delivery process, to the time immediately after the overvoltage is switched on.

3.3. II. General Case – "Discharge with Diffusion in both Phases"

We formulate the mathematical problem whose solution gives the time course for the more general case. The diffusion equations apply to both discharge-determining components. The charge transfer current provides the boundary conditions at the phase boundary. We thus get:

$$\frac{\partial c_{0x}}{\partial t} = \mathscr{D}_{0x}\cdot\frac{\partial^2 c_{0x}}{\partial x^2}\,; \quad \frac{\partial c_r}{\partial t} = \mathscr{D}_r\cdot\frac{\partial^2 c_r}{\partial x^2} \tag{3.6}$$

$$t = 0\ : c_{0x} = {}_0c_{0x}\,; \quad c_r = {}_0c_r \tag{3.7a}$$

$$x = \infty\ : c_{0x} = {}_0c_{0x}\,; \quad c_r = {}_0c_r \tag{3.7b}$$

$$x = 0\ : n\cdot\mathscr{F}\cdot\mathscr{D}_{0x}\cdot\frac{\partial c_{0x}(t)}{\partial x} = -j = n\cdot\mathscr{F}\cdot\mathscr{D}_r\cdot\frac{\partial c_r(t)}{\partial x}\,. \tag{3.7c}$$

---

[3] Better called: diffusion polarization, [19].

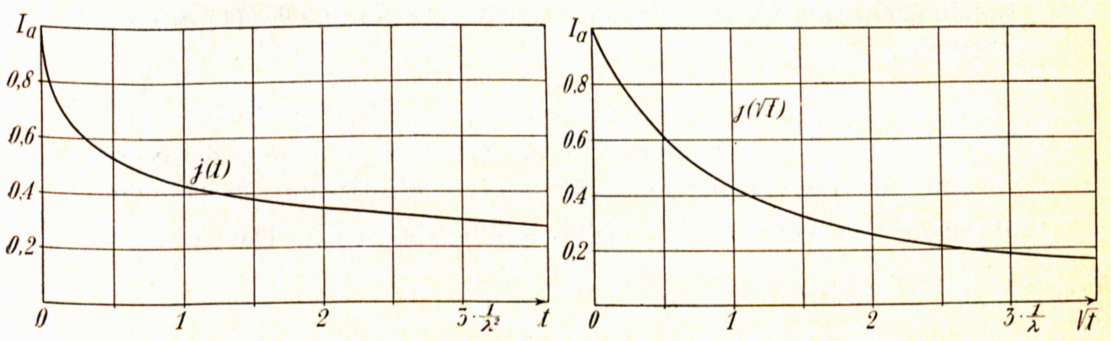

Figure 3.1.: Temporal sequence of the charge transfer current during the potentiostatic switch-on process

For j Equation 3.2 is used. From this system of differential equations one can calculate $c_{0x}(t)$ and $c_r(t)$ at the phase boundary. This is most easily accomplished by using the LAPLACE transform, a method that was first used to solve complicated diffusion problems in electrode processes by KOUTECKY and BRDICKA, [25], and subsequently proved to be very fruitful, [7, 21]. The solution to the above problem is briefly outlined in Part III.
We finally get the following result for the current curve over time:

$$j(t) = I_a(\eta) \cdot e^{\lambda^2 \cdot t} \cdot \operatorname{erfc}\left(\lambda \cdot \sqrt{t}\right) \tag{3.8}$$

$$\lambda = \frac{j_0}{n \cdot \mathscr{F}} \cdot \left\{ \frac{e^{\alpha \cdot \frac{n}{\Phi} \cdot \eta}}{{}_0c_r \cdot \sqrt{\mathscr{D}_r}} + \frac{e^{-(1-\alpha) \cdot \frac{n}{\Phi} \cdot \eta}}{{}_0c_{0x} \cdot \sqrt{\mathscr{D}_{0x}}} \right\} \tag{3.9}$$

(For $I_a(\eta)$ see Equation 3.3).
The time course for $\frac{j(t)}{I_a}$ is shown in Figure 3.1 plottet against t $\left(\text{in the unit } \frac{1}{\lambda^2}\right)$ and against $\sqrt{t}$ $\left(\text{in the unit } \frac{1}{\lambda}\right)$ respectively.
The quickest way to get a clear overview of the curve is to look at some limiting cases and approximate solutions of Equation 3.8:

(a) *Short time intervals*: $\lambda \cdot \sqrt{t} \ll 1$:
The following approximation holds:

$$j(t) \approx I_a(\eta) \cdot \left(1 - 2 \cdot \frac{\lambda}{\sqrt{\pi}} \cdot \sqrt{t}\right) . \tag{3.8a}$$

The limiting case $t \to 0$ results as expected:

$$j(t \to 0) = I_a(\eta) . \tag{3.10}$$

(b) *long time intervals*: $\lambda \cdot \sqrt{t} \gg 1$:
As an approximation one now gets, [24]:

$$j(t) \approx I_a(\eta) \cdot \frac{1}{\sqrt{\pi} \cdot \lambda \cdot \sqrt{t}} = \frac{\Lambda}{\sqrt{\pi}} \cdot \frac{1}{\sqrt{t}} \tag{3.8b}$$

with[4]

$$\begin{aligned}\Lambda = \frac{I_a(\eta)}{\lambda(\eta)} &= n \cdot \mathscr{F} \cdot \frac{1 - e^{-\frac{n}{\Phi}\cdot\eta}}{{}_0c_{0x} \cdot \sqrt{\mathscr{D}_{0x}} + e^{-\frac{n}{\Phi}\cdot\eta} \cdot {}_0c_r \cdot \sqrt{\mathscr{D}_r}} \\ &\quad \cdot {}_0c_{0x} \cdot {}_0c_r \cdot \sqrt{\mathscr{D}_{0x} \cdot \mathscr{D}_r}\,. \end{aligned} \tag{3.11}$$

The discharge rate –characterized by j_0 and α– is no longer included in this relationship. It is the time course with pure diffusion polarization in both phases in full analogy to the previously mentioned Equation 3.5. The same limit law applies to vanishing discharge inhibition, i.e. $j_0 \to \infty$.
We see that for ${}_0c_r \gg {}_0c_{0x}$, i.e. negligible concentration polarization for the reducing component, Equation 3.11 turns into Equation 3.5.

(c) *Time of transition to diffusion-determined time course*:
What is also of interest is the point in time τ at which the current flow changes from proportionality according to $\sqrt{t}$ (discharge as main point) to $\sim \frac{1}{\sqrt{t}}$ (diffusion as main point). There, e.g. $\lambda \cdot \sqrt{\tau} = 1$, so:

$$\tau = \frac{1}{\lambda^2}\,. \tag{3.12}$$

At the point of time τ the current has fallen according to Equation 3.8 to:

$$j(\tau) = 0.427 \cdot I_a(\eta)\,. \tag{3.13}$$

---

[4] Where: $\mathrm{erfc}(y) = 1 - \mathrm{erf}(y) = 1 - \frac{2}{\sqrt{\pi}} \cdot \int_0^y e^{-\xi^2}\,\mathrm{d}\xi$.

3.4. The Involvement of Fast, Upstream Reactions

We would also like to address the question of what the time current curve looks like in systems in which upstream reactions are involved in the electrode process or the discharge reaction itself is a process of a higher reaction order, as one would expect, for example, in the discharge of complex ions. In the most general case, taking into account the contribution of upstream reactions requires a separate calculation, which we will return to in a later communication. However, in a special case that seems to occur frequently, one can obtain statements about such cases analogous to the previous considerations. This is possible if the discharge rate is small compared to the reaction rate, so that the reaction equilibrium can practically always be reached. The discharge shall in addition pass through an intermediate substance that is only present in a low concentration compared to the concentration of the reactants with which it is in equilibrium. Such a reaction mechanism has been demonstrated for the discharge of complex ions in various systems, [15, 17].

In this case, the concentration of the discharge-determining intermediate determines the charge transfer current in the manner stated earlier, but its concentration itself is controlled by the diffusion of the reactants via the reaction equilibrium. To explain this, let us consider the following reaction example:

Discharge determining step:

$$\mathrm{M} + \nu\mathrm{X} \rightleftharpoons (\mathrm{MX}\nu)^{n+} + ne^- \, . \tag{3.14}$$

Upstream reaction:

$$[\mathrm{MX}\nu]^{n+} + (\mu - \nu) \cdot \mathrm{X} \rightleftharpoons [\mathrm{MX}\mu]^{n+} \, . \tag{3.15}$$

For the charge transfer current it now follows, [16]:

$$j = j_0 \cdot \left\{ \frac{c_\mathrm{M}}{{}_0c_\mathrm{M}} \cdot \left(\frac{c_\mathrm{X}}{{}_0c_\mathrm{X}} \right)^\nu \cdot e^{\alpha \cdot \frac{n}{\Phi} \cdot \eta} - \frac{c_\nu}{{}_0c_\nu} \cdot e^{-(1-\alpha) \cdot \frac{n}{\Phi} \cdot \eta} \right\} \tag{3.16}$$

with

$$j_0 = {}^0j \cdot {}_0c_\mathrm{M}^{(1-\alpha)} \cdot {}_0c_\mathrm{X}^{\nu \cdot (1-\alpha)} \cdot {}_0c_\nu^\alpha \, . \tag{3.17}$$

If the upstream reaction is fast, equilibrium exists:

$$\frac{c_\nu \cdot c_\mathrm{X}}{c_\mu} = K_{\nu\mu} = \frac{{}_0c_\nu \cdot {}_0c_\mathrm{X}}{{}_0c_\mu} \, . \tag{3.18}$$

If ${}_0c_\nu \ll {}_0c_\mu$, then for the transport process of the substance $[\mathrm{MX}_\mu]$ the differential equation according to Equation 3.6 with the boundary conditions according to Equation 3.7a to Equation 3.7c is applicable in the same way as it is formulated there for the oxidizing component. If we choose a large excess of the complexing agent: ${}_0c_\mathrm{X} \gg {}_0c_\mu$, its diffusion remains negligible[5]. The replacement of c_ν in Equation 3.16 by c_μ from Equation 3.18, after inserting it into the boundary condition Equation 3.7c, results in a complete analogy in the calculation of the concentration curve for c_μ in relation to the case discussed in Part III with $c_{0x}(t)$. Since $c(t)$ with our assumption according to Equation 3.18 is known and therefore $c_r(t)$ is also known, we immediately get the same result for the time-current curve as in Equation 3.8 and Equation 3.9. Only in Equation 3.9 the index $0x$ has to be replaced by μ and j_0 is now determined by Equation 3.17.

Under these conditions, one can develop approximate relationships analogously to the equations derived above. This will be important later for the analysis of the reaction mechanism.

---

[5] If this requirement is not met, a third diffusion equation for the complexing agent is added in Equation 3.6. The boundary condition Equation 3.7c acquires a non-linear form after inserting Equation 3.16. Then applying the LAPLACE transformation no longer leads to a valuable result.

4. Discussion and Conclusions about the Reaction Mechanism

4.1. Determination of the "Initial Potential-Current Curve"

Extrapolation of the course of current to $t \to 0$ results in the initial current $I_a(\eta)$ according to Equation 3.8a and Equation 3.10. This is the current that would flow constantly if no changes in concentration occurred. If this initial current at different overvoltages is determined, it is possible to construct a current-voltage curve that does not contain any concentration polarization. We want to call this current-voltage curve, which is only determined by the charge transfer inhibition, the "initial current-voltage curve" or the current-voltage curve for "pure discharge". The characteristic kinetic quantities j_0 and α can be derived directly from it.
Whether an extrapolation is experimentally possible depends essentially on j_0, the equilibrium concentration and the applied overvoltage, as can be seen from Equation 3.12. The experimental conditions to be discussed in the following communication assume, e.g. $\tau > 0.05$ seconds. For smaller values of τ one can still use Equation 3.13 to make a rougher estimate.
An appropriate choice of ${}_0c$ and η allows some kind of adaptation to the system. In the case of a rapid transition to the diffusion-determined time-current curve, the best way seems to be to compare the measured curve with the theoretical curve for pure diffusion polarization according to Equation 3.8b. To do this, it is convenient to plot the current curve against $\frac{1}{\sqrt{t}}$. This comparison is done in Figure 4.1. Current and time are plotted there in reduced units: $\frac{j(t)}{I_a}$ according to Equation 3.8 or Equation 3.8b against $\frac{1}{\lambda \cdot \sqrt{t}}$. For further clarification, the limiting case: "Pure discharge" is included in Figure 4.1a. Below the representation of the time-current curve the ratio of $j_{\mathrm{DE}}(t)$ for diffusion plus discharge according to Equation 3.8 to $j_{\mathrm{D}}(t)$ in the case of pure diffusion according to Equation 3.8b: $Q = \frac{j_{\mathrm{DE}}}{j_{\mathrm{D}}}$ versus $\frac{1}{\lambda \cdot \sqrt{t}}$ is plotted in Figure 4.1b.
For example, if the measured curve is plotted against $\frac{1}{\sqrt{t}}$, the curve for pure diffusion can easily be extrapolated from the measuring points at large t. Comparing the measured curve with the extrapolated curve gives the quotient Q at certain points in time. To do this, one can take the corresponding quotient $\frac{1}{\lambda \cdot \sqrt{t}}$ from Figure 4.1 and in turn from this λ and I_a.

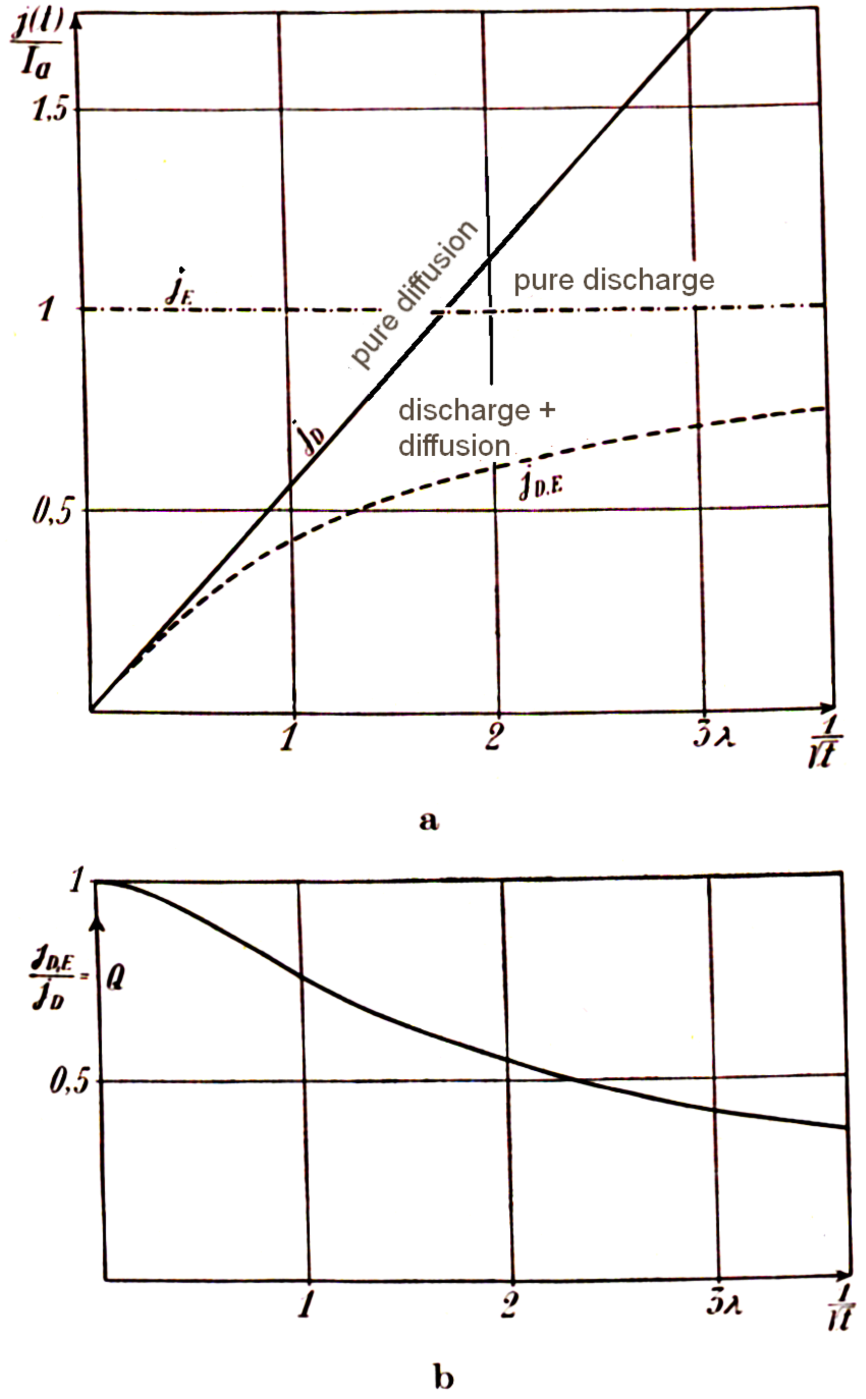

Figure 4.1.: Comparison of the time-current curve when coupling discharge inhibition and subsequent delivery through diffusion with the limiting cases: *Pure diffusion* and *Pure discharge.*

4.2. Determination of the Exchange Current Density and the Charge Transfer Coefficient

As has just been said, the exchange current density and the charge transfer coefficient can be calculated from the initial current-voltage curve. For j_0 it is sufficient to know the slope of this current-voltage curve at the equilibrium potential. From Equation 3.3 one immediately obtains:

$$\left(\frac{\mathrm{d}I_a}{\mathrm{d}\eta}\right)_{\eta=0} = \frac{n}{\Phi} \cdot j_0 = \frac{1}{R_\mathrm{D}}\,, \tag{4.1}$$

where R_D is the charge transfer resistance.
To measure the inclination $\left(\frac{\mathrm{d}I_a}{\mathrm{d}\eta}\right)_{\eta=0}$ one only needs to determine the initial current at very small overvoltages (about ±2 mV to 5 mV), where the current-voltage curve can be approximated linearly.
The charge transfer coefficient α results from the symmetry relations of the curve. If α should be determined with any precision, one has to move further away from equilibrium. The best way is to get α from comparing the measured initial current-voltage curve with one theoretically calculated according to Equation 3.3, whereby it is most convenient to use the j_0 determined in the manner given above to plot a relative initial current density:

$$\frac{I_a(\eta)}{j_0} = e^{\alpha \cdot \frac{n}{\Phi} \cdot \eta} - e^{-(1-\alpha) \cdot \frac{n}{\Phi} \cdot \eta} = \Psi\left(\alpha, \frac{\eta}{\Phi/n}\right)$$

against a relative overvoltage $\frac{\eta}{\Phi/n}$. This reduced representation of the initial current-voltage curve is recorded in Figure 4.2 with α as a parameter[1].
If j_0 is large, it will often no longer be possible to measure the initial current at larger η. Then, to determine α, one can use the method developed earlier in another context, in which the dependence of the exchange current density on the concentration of the discharge-determining components is used, [19, 12].

4.3. Analysis of the Reaction Mechanism

If extrapolation to the initial current is possible even in more complicated reactions, which requires that the reaction equilibrium is reached fast and that inhibited discharge occurs, as shown previously, conclusions can be drawn about the discharge determining step. One way to do this is to calculate the exchange current density

---

[1] α can also be obtained very quickly by calculating the anodic and cathodic initial partial currents according to Equation 4.6, whose logarithmic plot against η should result in a straight line according to TAFEL's equation, the slope out of which can be derived in the usual way α or $(1-\alpha)$.

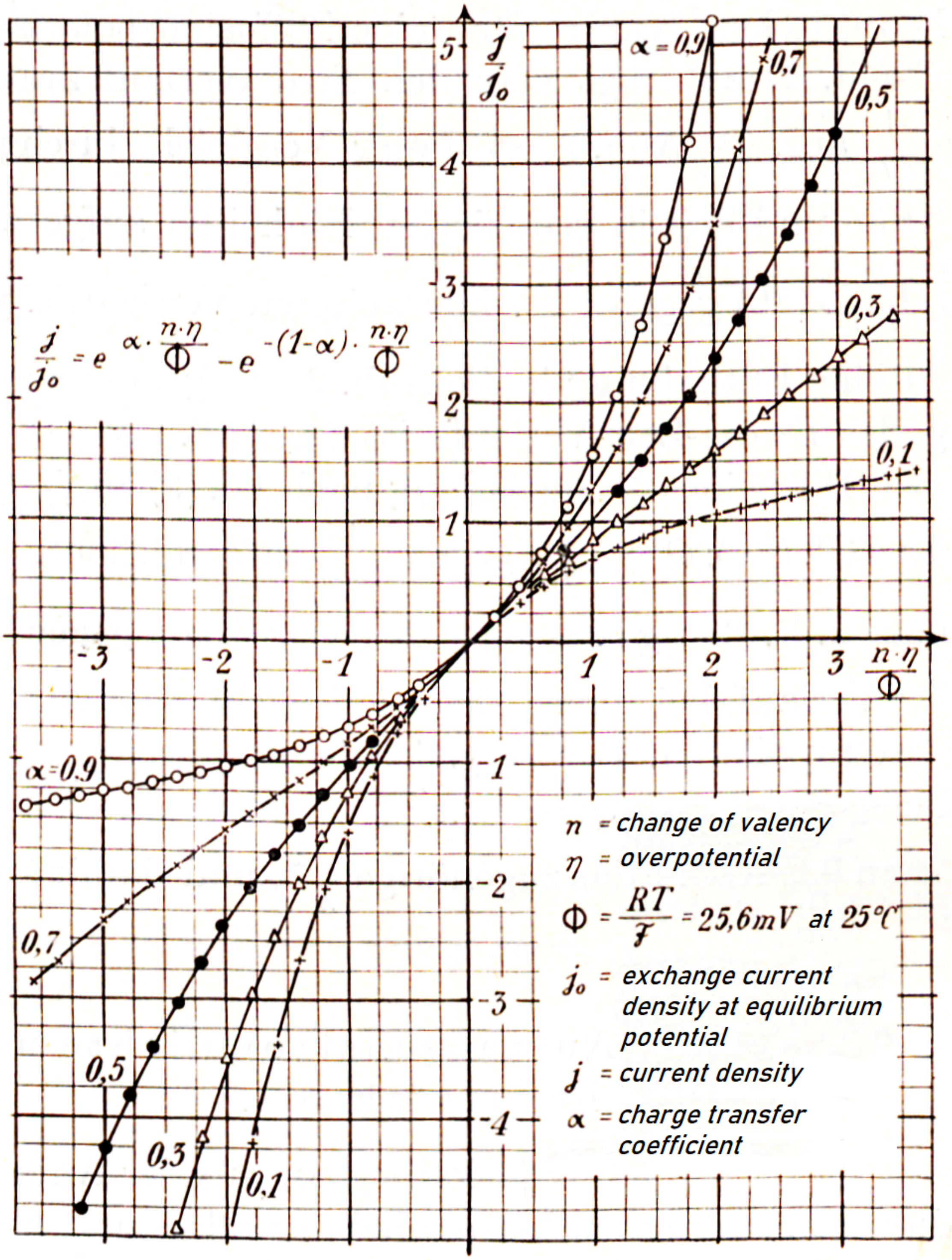

Figure 4.2.: Current-voltage curves for pure discharge in a reduced representation with charge transfer coefficient α as a parameter

and measure its dependence on the concentration of the reactants involved. The discharge mechanism of complex ions is mainly dependent on the concentration of the complexing agent, as discussed in detail earlier, [16].

However, the potentiostatic method opens up a new possibility that directly follows the usual procedure in reaction kinetics and is therefore particularly transparent and clear. We want to explain this method using the example of discharging a complex ion according to the reaction types in Equation 3.14 and Equation 3.15. It can be applied analogously to any electrode reaction that meets the requirements mentioned at the beginning.

To more clarify this method, we write the kinetic Equation 3.16 for the charge transfer current again in a slightly different formulation:

$$\begin{aligned} j &= k^+ \cdot c_\mathrm{M} \cdot c_\mathrm{X}^\nu \cdot e^{\alpha \cdot \frac{n}{\Phi} \cdot \varepsilon} - k^- \cdot c_\nu \cdot e^{-(1-\alpha) \cdot \frac{n}{\Phi} \cdot \varepsilon} \\ &= j^+ \qquad\qquad\qquad\qquad - j^- \end{aligned} \tag{4.2}$$

where the electrode potential ε shall now be related to a specific reference electrode. k^+ and k^- depend on the choice of this reference point. This equation applies to the initial current using the equilibrium concentrations.

We see that at constant potential the anodic and cathodic initial partial currents I_a^+ and I_a^- are related to the concentrations in the following way:

$$\begin{aligned} I_a^+(\varepsilon = \text{const.}) &\sim {}_0c_\mathrm{M} \cdot {}_0c_\mathrm{X}^\nu \\ I_a^-(\varepsilon = \text{const.}) &\sim {}_0c_\nu \,. \end{aligned} \tag{4.3}$$

The reaction order of the discharge step in relation to this component results directly from the dependence of the initial partial currents on the concentration of the discharge-determining components, here in particular of the anodic initial partial current on the concentration of the complexing agent. For evaluation it is advisable to use the form:

$$\left(\frac{\partial \log \left(I_a^+\right) (\varepsilon = \text{const.})}{\partial \log \left({}_0c_\mathrm{X}\right)} \right)_{{}_0c_\mathrm{M} = \text{const.}} = \nu \,. \tag{4.4}$$

The analogy to normal reaction kinetics is perfect here because the influence of the electrical potential on the reaction rate remains constant.

If the overvoltage is known, the initial partial currents can be easily calculated from the measured initial current I_a. Because the following relationship applies (easily derived from Equation 3.3):

$$\frac{I_a^+}{I_a^-} = e^{\frac{n}{\Phi} \cdot \eta} \,. \tag{4.5}$$

With $I_a = I_a^+ - I_a^-$ we get from Equation 4.5[2]:

$$I_a^+ = \frac{I_a}{1 - e^{-\frac{n}{\Phi} \cdot \eta}} \quad \text{bzw.} \quad I_a^- = -\frac{I_a}{1 - e^{\frac{n}{\Phi} \cdot \eta}} \,. \tag{4.6}$$

---

[2] Note that I_a can be positive and negative.

To analyze the reaction mechanism, one must measure the initial current at the same potential for different concentrations of a specific reactant. For complex ions, it is recommended to measure the anodic formation rate, which almost corresponds to the anodic partial current in the case of more inhibited discharge and larger overvoltage, and which time sequence is particularly little influenced by the rate of upstream reactions.

4.4. Comparison With Other Methods

The method proposed here for measuring j_0 and α is largely analogous to the evaluation of measurements of the polarization impedance in corresponding systems, [28, 10, 11, 14]. There, too, an extrapolation procedure was used to eliminate concentration changes. The extrapolation there to the frequency ∞ corresponds here to the extrapolation to $t \to 0$. In both cases we get the charge transfer resistance R_D. The applicability of both methods is limited by the involvement of double-layer charging, in which nullifies all too short-term processes. When the exchange current density is high and adjustment processes are quick, the alternating current method is more sensitive and therefore preferable. However, the potentiostatic method is particularly useful in cases where alternating current measurement fails (e.g. when the balance is imperfectly reached due to high charge transfer inhibition, i.e. very small j_0). In the latter case, by choosing a sufficiently large overvoltage, discharge speeds can be set so high that the power consumption due to secondary processes on the electrode becomes negligible and decay times for the switch-on process are reached in which uncontrollable disturbances caused by convection and the like are not yet noticeable. These extensive adaptation options to the kinetic conditions are a key advantage of the potentiostatic method.

The potentiostatic method is also an excellent addition to the methods previously used when investigating the reaction mechanism of more complicated processes. In turn, it can be applied most advantageously to systems with greater discharge inhibition. We have also seen that evaluating the measurements can be much easier.

Compared to all investigations in which stationary current-voltage curves are recorded, this method has the great advantage that the current only flows through the electrode for a very short time. The changes in the electrode surface, which are inevitably associated with the current flow on solid electrodes, can therefore be limited to a minimum. The method is therefore particularly recommended for investigations on solid electrodes.

From the Max-Planck-Institute for physical chemistry, Göttingen.

Part II.

On electrolysis at constant potential. II. Studies on the kinetics of the deposition of simple zinc and complex silver ions

With 11 figures in text. (Received on 23.12.54.)

1. Abstract

The considerations presented in Part I of this study are applied here to various electrode processes. The measurements on the Zn-Amalgam/$Zn^{2+} \cdot aq$ system, whose kinetics have already been studied in detail, [15], serve to test the applicability. The measurements on the system Ag/$[Ag(NH_3)_2]^+$ and Ag/$[Ag(CN)_x]^{(x-1)-}$ were able to clarify the kinetics of the relevant electrode processes.

2. Experimental Setup

2.1. The Potentiostat

The task of keeping the electrode potential constant using a suitable control circuit has already been addressed on various occasions. A comprehensive overview of the arrangements used can be found in LINGANE, [27]. However, the potentiostats described there are always discontinuous control circuits with a control time that hardly goes below 0.1 s. Since we were particularly interested in the current progression over time immediately after the desired potential was set, we only considered devices with much faster regulation. One such potentiostat with continuous control which has been developed is from HODGKIN, HUXLEY and KATZ, [22] as well as from SCHOEN and STAUBACH, [29]. We used an arrangement that works on the same principle and which is briefly described here. It was built with the support of the last-mentioned authors, for which we would like to express our appreciation at this point.
Figure 2.1 shows the basic circuit diagram of the potentiostatic arrangement. The most important part is a DC voltage amplifier that works in a push-pull circuit as a differential amplifier, which delivers through its power amplifier the current for electrolysis.

The differential voltage $\Delta\varphi$ is effective at the input of the amplifier, which is composed of the potential difference ε between the measuring electrode E_1 and the electrode for comparison E_3, as well as the two adjustable voltages U_k and U_p:

$$\Delta\varphi = \varepsilon + U_k + U_p \,. \tag{2.1}$$

Before starting the experiment, $\Delta\varphi$ is made zero with the polarization voltage circuit switched off ($U_p = 0$), i.e. the potential difference in the de-energized state: $\varepsilon = \varepsilon_0$ is compensated by U_k. Since an electron tube only delivers a direct current in one direction, it is necessary to set the device to a favorable operating point in the middle of the control range at $\Delta\varphi = 0$ and to compensate the direct current J_R delivered by the device with a countercurrent J_0, so that at $\Delta\varphi = 0$, $J = 0$ applies to the measurement object.
If we now apply an additional polarization voltage U_p to the input, a large current J will initially flow in the polarization circuit. In the linear amplification range, its amount is given by the gain V of the DC voltage amplifier and the slope S of the current-supplying output tubes:

$$J = -V \cdot S \cdot \Delta\varphi \,. \tag{2.2}$$

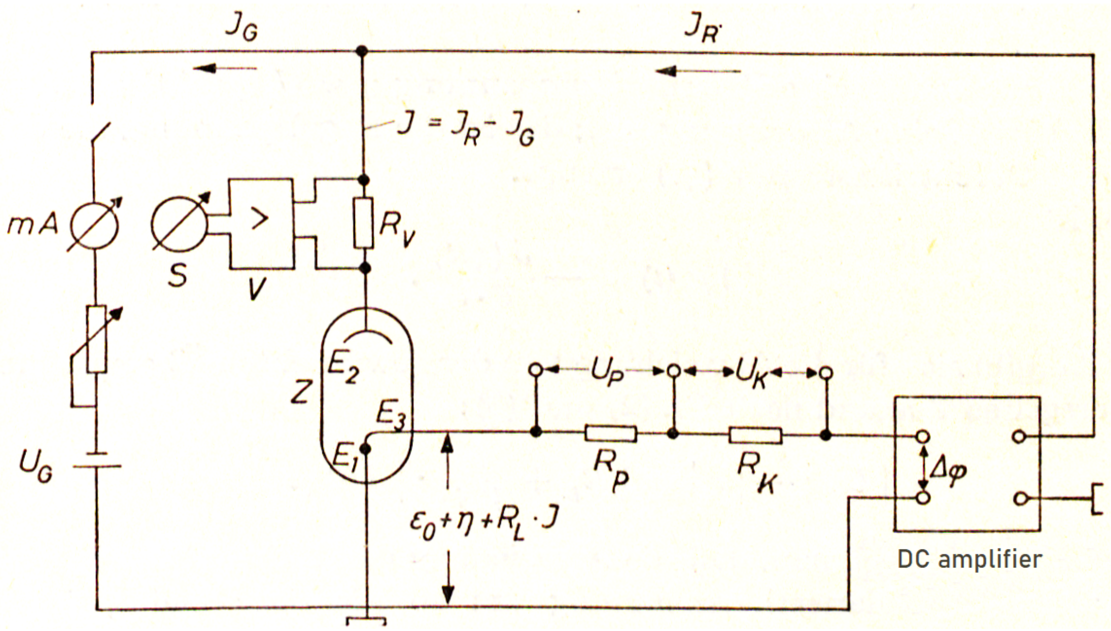

Figure 2.1.: Block diagram for electrolysis at constant potential with electronic potentiostat. E$_1$ = measuring electrode. E$_2$ = counter electrode. E$_3$ = electrode for comparison . S = loop oscillograph. Z = electrolysis cell. V = DC amplifier

$\frac{1}{VS}$ is the effective resistance of the potentiostat. At the beginning $\Delta\varphi = U_p$. The amplifier will usually be overdriven, so that a constant current initially flows. Due to the large current, the electrode is polarized very quickly, with increasing overvoltage: $\eta = \varepsilon - \varepsilon_0$, the effective voltage $\Delta\varphi$ drops almost to zero (as a result of the current degeneration, the generated voltage at the electrolysis cell Z always has the opposite sign of U_p):

$$|\Delta\varphi(t)| = |U_p| - \{|\eta(t)| + R_L \cdot |J(t)|\} \ . \tag{2.3}$$

Here R_L is a part of the electrolyte resistance recorded by the Luggin capillary E$_3$.
So the desired polarization voltage $\eta \approx U_p$ is set practically very quickly up to a deviation $\Delta\varphi_r$; this is the control voltage that generates the charge transfer current $J(\eta, t)$ belonging to η.
According to Equation 2.3 it follows:

$$\Delta\varphi_r(t) = -\frac{J(\eta, t)}{V \cdot S} \ . \tag{2.4}$$

For the deviation from the desired overvoltage U_p in the balanced state we get according to Equation 2.2 and Equation 2.3:

$$|U_p| - |\eta| = \left(R_L + \frac{1}{VS}\right) \cdot |J(t)| \ . \tag{2.5}$$

From Equation 2.5 it can be seen that the smaller the effective resistance of the potentiostat: $R_L + \frac{1}{VS}$, the lower the deviation of the electrode potential from the desired polarization voltage. Since R_L cannot be made arbitrarily small, there results from this point of view a limit for a meaningful gain of the device as

$$\frac{1}{VS} \ll R_L\,. \tag{2.6}$$

On the other hand, the internal resistance of the potentiostat also determines the charging time τ of the electrode with its double-layer capacitance C. The second boundary condition follows from $\tau = \frac{C}{VS}$:

$$\frac{1}{VS} \leq \left(\frac{\tau}{C}\right)_{\max}\,. \tag{2.7}$$

However, there is a lower limit to the charging time due to the frequency response of the entire arrangement. The width of the frequency band must be selected according to the stability requirements of the control circuit. This question has been discussed in detail by BODE, [1], and TERMAN, [32]. In any case, one must ensure by installing suitable attenuators that the gain drops below 1 for all frequencies at which the phase shift between the input and output signal exceeds 180°, i.e. the negative feedback becomes a positive feedback. Since the input impedance plays a major role, this can only be achieved on a case-by-case basis by adaptation to the respective measurement object.

From these considerations it follows that it does not make sense to increase the gain of the device too high. In any case, the device must be adapted to the currents that occur. Oversizing is just as harmful as the opposite. The high capacitances occurring in the electrode impedance, in connection with the conditions just mentioned, limit the achievable control times to approximately 1×10^{-4} s, so that a frequency-accurate reproduction of the switch-on process seems only possible up to a bandwidth of a few kHz. Excessively rapid changes in the charge transfer current can therefore no longer be recorded.

The amplifier we used is shown in Figure 2.2. It had an amplification factor of around 2000 and a frequency range up to 50 kHz, which, however, has to be limited to around 10 kHz to stabilize the device due to the large capacitances in the measurement object. The current was measured using a Siemens loop oscillograph (S) with a DC amplifier (V) connected in front of it (see Figure 2.1). Since the resistor R_V, which is used to measure the current, has little influence on the potentiostatic arrangement[1], it can be varied without difficulty and adjusted to the respective current flow.

2.2. The Measuring Cells

The measurements on Zn-Amalgam were carried out on the hanging amalgam drop in an arrangement described elsewhere, [15]. The drop surface was approximately 4×10^{-2} cm^2. Our studies on solid electrodes were carried out in a glass apparatus as shown in Figure 2.3. An Ag wire was melted into a glass tube and the melting spot of the wire was sealed from the inside with polyethylene. The free end of the wire was about 1 cm long. Its tip was

---

[1] R_V is only included in the input negative feedback and therefore influences the frequency response somewhat.

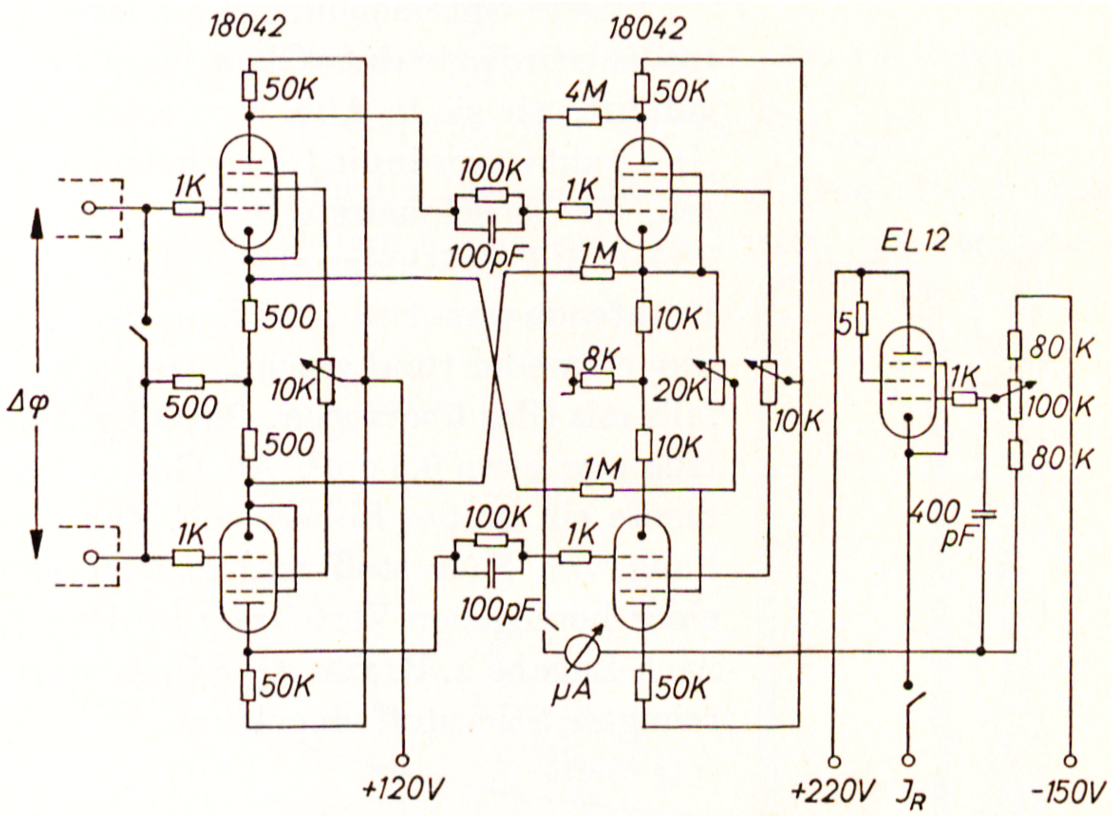

Figure 2.2.: Two-stage DC amplifier with coupled output stage

either melted round or also covered with glass. The surface area here was approximately 0.3 cm^2. A large silver sheet served as the counter electrode. Purified nitrogen was introduced to drive off oxygen and to produce a homogeneous distribution in the solution after adding, for example, Ag salts.

2.3. Preparation of the Solutions. Pretreatment of the Electrodes

The silver salt solution was prepared by dissolving silver sheet in $HClO_4$ to which H_2O_2 was added. After the perchloric acid had been consumed, the H_2O_2 was decomposed by boiling. The same procedure could be used for the $Zn(ClO_4)_2$. As a foreign electrolyte, we used a 1 N $NaClO_4$ solution, which was obtained by neutralizing $HClO_4$ with NaOH. *pa*-chemicals and double-distilled water served as starting materials.
The Zn-Amalgam was prepared by cathodic deposition of Zn^{2+} from $Zn(ClO_4)_2$ solution on mercury. The amalgam contained about 1 mole percent zinc.
The silver electrodes were polished using a chemical process before each measurement, [18]. The electrodes were then rinsed in perchloric acid and double-distilled water. Fine silver (Heraeus 99.99 %) was used as the silver metal.

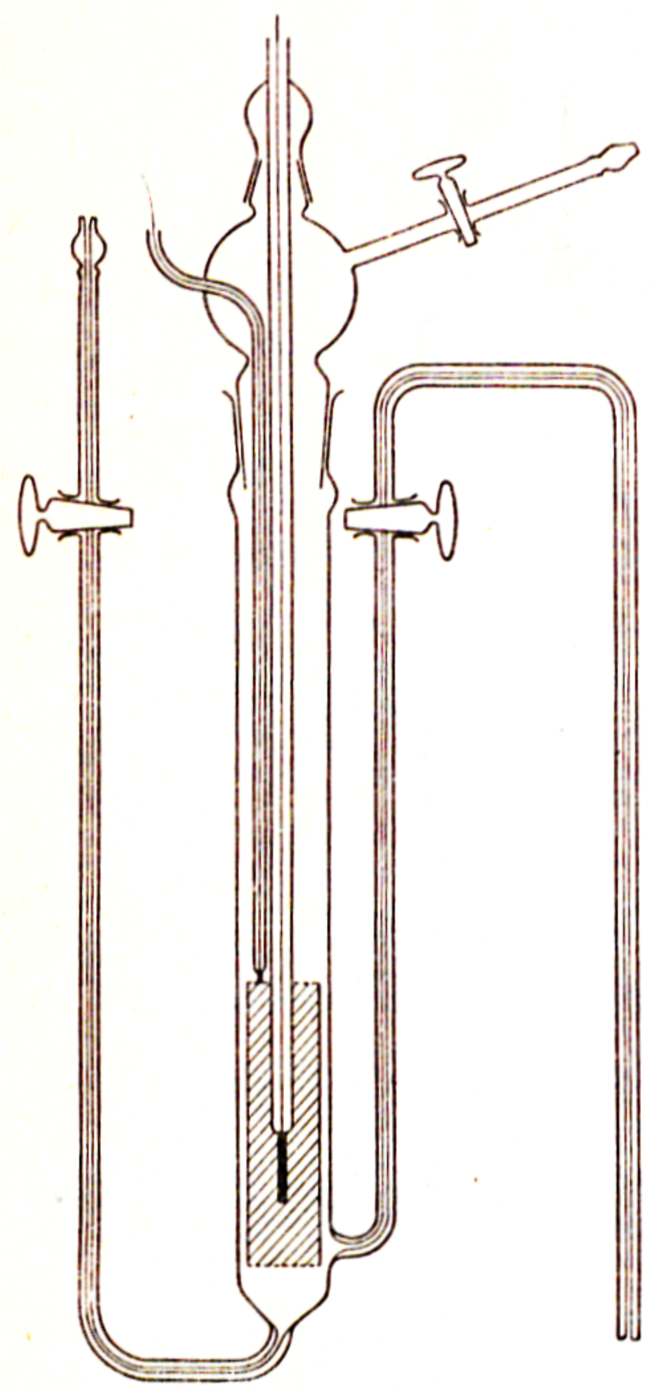

Figure 2.3.: Electrolysis cell for polarization measurements on solid electrodes

3. Discharge of Simple Zn^{2+}-Ions on Zn-Amalgam

3.1. Time-Current curve

A system in which only a simple coupling of charge transfer and diffusion polarization is to be expected is suitable for checking the formulæ for the time-current curve derived in the theoretical part. This is the case with zinc amalgam in a simple Zn^{2+} ion solution. The time-current curve $j(t)$ on a zinc-amalgam drop at potentiostatic polarization of the Zn-Amalgam/$Zn(ClO_4)_2$ system in 1 M $NaClO_4$ solution is shown for two different overvoltages ($\eta = -20\,\mathrm{mV}$, $\eta = -60\,\mathrm{mV}$) in Figure 3.1. The curve corresponds quite well to the curve calculated in Figure 3.1a or Equation 3.8 of Part I of this work.

In our theoretical considerations, we found that for short periods of time after the overvoltage is switched on, the discharge is determinant and a linear drop in the current according to $\sqrt{t}$ is to be expected. After the time τ, which is given by the relation (Equation 3.14)

$$j(\tau) = 0.427 \cdot I_a$$

the diffusion rate should become determinant and the curve should change into a course $\propto \frac{1}{\sqrt{t}}$. To compare this with theory, we have again plotted the curves of Figure 3.1 in Figure 3.2 against $\sqrt{t}$ and $\frac{1}{\sqrt{t}}$. The junction with the linear progression with $\frac{1}{\sqrt{t}}$ is clearly visible. As expected, the course of the curve deviates earlier from the $\sqrt{t}$ path with the larger polarization voltage and also moves more quickly into the $\frac{1}{\sqrt{t}}$ path of pure diffusion. With a larger negative current, the electrolyte in front of the electrode becomes depleted of Zn^{2+} ions more quickly; Diffusion therefore determines the speed of the gross reaction earlier.

The path with $\sqrt{t}$ for small times can also be seen, although less clearly. The latter is because the evaluation of the recordings for times $t \ll 1 \times 10^{-1}\,\mathrm{s}$ became difficult with the oscillograph loop used. With our arrangement we were at the limit of the resolvability of the switch-on process because the current drop caused by diffusion occurs too quickly. However, the resolution of the time course achieved, which can still be improved, was sufficient to determine the size of the initial current $j(t = 0) = I_a(\eta)$ and thus the speed of the pure discharge reaction by extrapolation for $t \to 0$ also with sufficient accuracy.

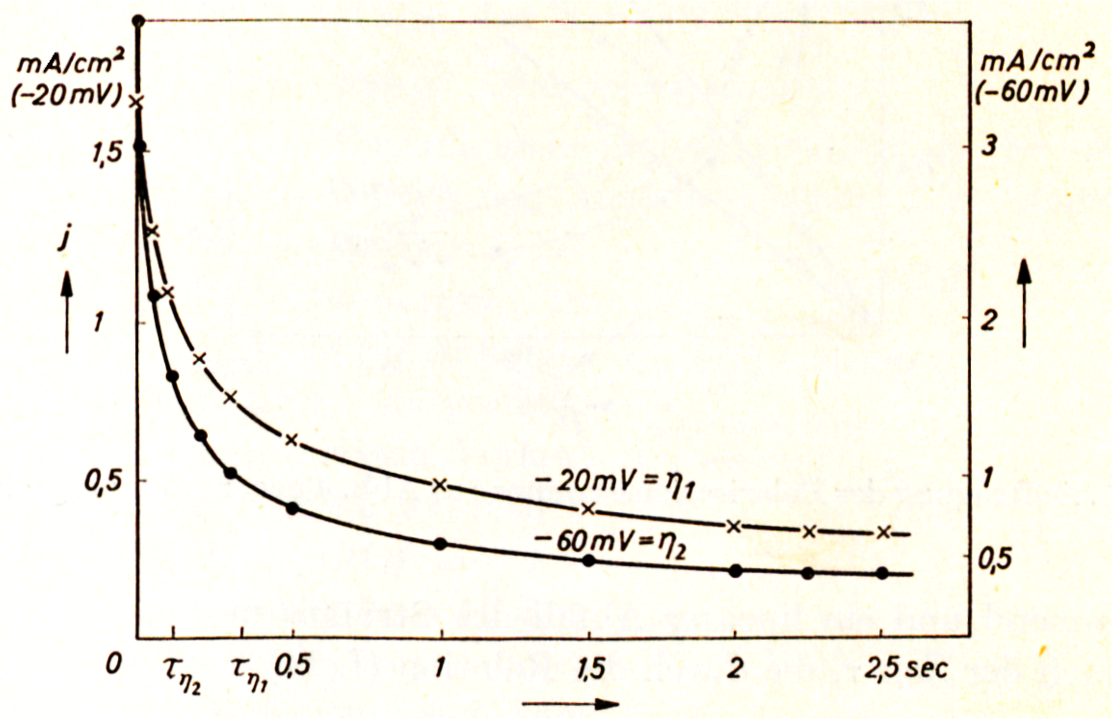

Figure 3.1.: Time-current curve with potentiostatic polarization on Zn-Amalgam/Zn^{2+} in 1 N $NaClO_4$ solution as a foreign electrolyte. Zn^{2+} concentration: 2.1×10^{-3} M. The left ordinate label refers to $\eta = -20\,\mathrm{mV}$, the right to $\eta = -60\,\mathrm{mV}$

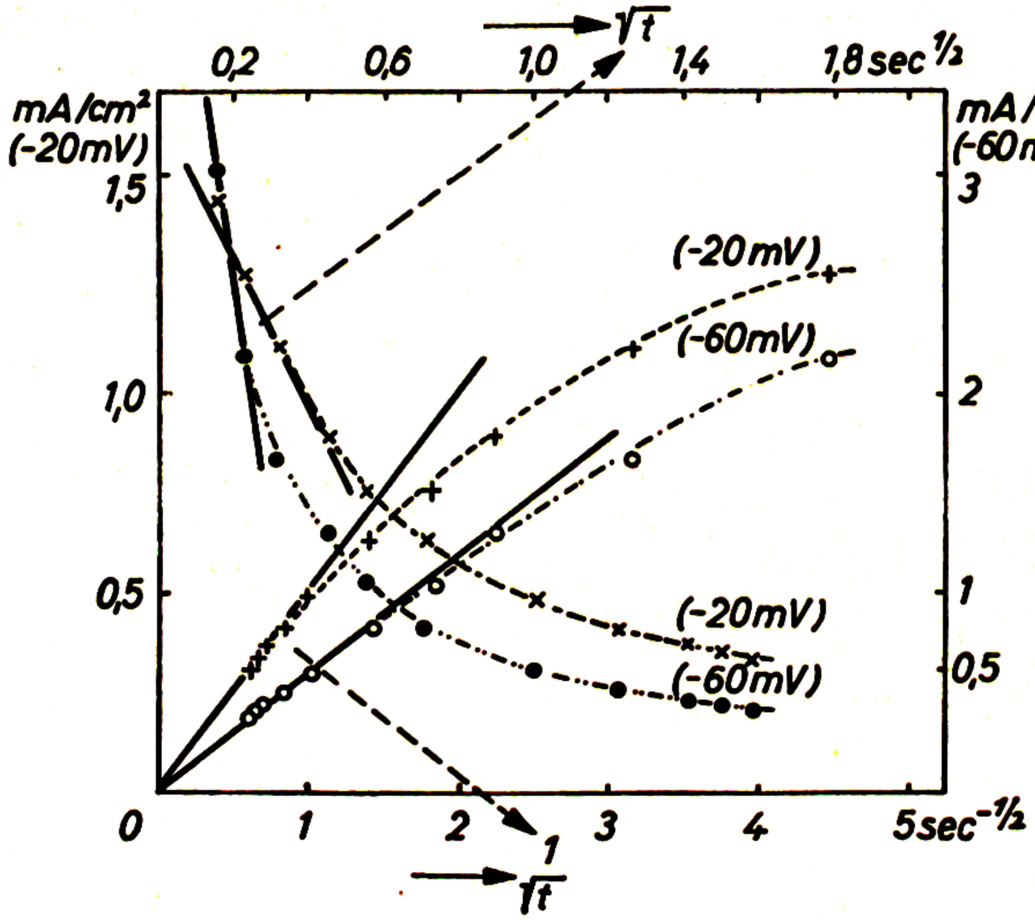

Figure 3.2.: Plot of the polarization current from Figure 3.1 against $\sqrt{t}$ and against $\frac{1}{\sqrt{t}}$

3.2. Determination of Kinetic Data

a) *"Pure" time-current curve.*

According to the explanations in Part I, the current-voltage curve caused solely by discharge inhibition is obtained by determining the initial current I_a at various overvoltages. An initial current-voltage curve obtained in this way is shown in Figure 3.3. The highly asymmetrical course indicates a charge transfer coefficient α that is significantly different from 0.5.
When evaluating the current curve over time to determine the initial current strength, there was no significant difference between a linear extrapolation of the initial peak of the current against $\sqrt{t} \to 0$ and the method explained in Part I by comparison with that course for pure diffusion.

b) *Calculation of j_0 and α.*

The exchange current density j_0 and the charge transfer coefficient α are clearly determined by the shape of the current-voltage curve solely, as can be seen from Equation 3.3. According to Equation 4.1 we immediately get j_0 from the slope at the equilibrium potential, which in our example results from Figure 3.3:

$$j_0 = 2.1\,\mathrm{mA\,cm^{-2}}\,.$$

We want to determine the value α by comparing the measured net current-voltage curve with one calculated according to Equation 3.3. The dashed curve of Figure 3.3 corresponds to the theoretical curve assuming $\alpha = 0.7$. The good agreement with the measuring points throughout the entire range shows that we have really obtained the current-voltage curve of pure discharge inhibition through the above extrapolation procedure. The small deviations at high overvoltage are probably due to the insufficient performance of the potentiostat used. According to the measurements obtained previously, [15], under similar conditions using the AC method, one should expect the following values for α and j_0 at the same concentrations:

$$\alpha = 0.76 \quad \text{and} \quad j_0 = 1.7\,\mathrm{mA\,cm^{-2}}\,.$$

The values obtained here therefore agree satisfactorily within other comparability.

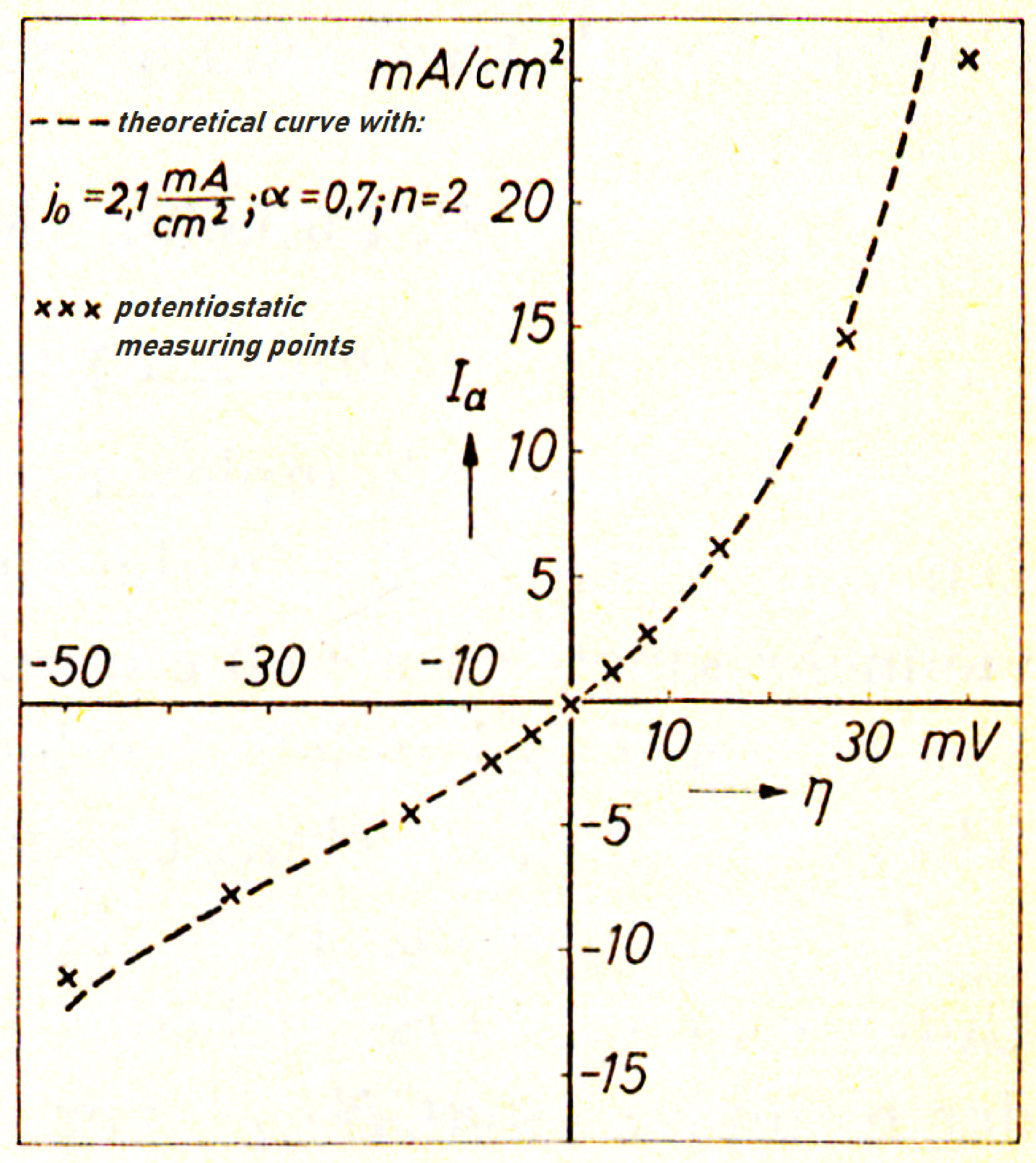

Figure 3.3.: Initial current-voltage curve on Zn-Amalgam/Zn^{2+} in 1 M $NaClO_4$ solution at 0 °C. Equilibrium potential: −1086 mV versus calomel. Zn^{2+}-concentration: 6×10^{-3} M

4. Discharge of complex Ag^{+} Ions

4.1. Complexes with Cyanide

The discharge of complex ions generally does not occur via the previous decay into the simple hydrated ions; rather, it must be treated kinetically as a direct, higher molecular reaction at the phase boundary, [17]. This is also confirmed by the studies described here on solid silver electrodes.

A number of different complexes occur in cyanide solution. Under our experimental conditions, the complex $[\mathrm{Ag(CN)_3}]^{2-}$ was predominantly present in the solution.

When the discharge-determining step is:

$$\mathrm{Ag}^{+} + \nu \mathrm{CN}^{-} \rightleftharpoons \mathrm{Ag(CN)}_{\nu}^{(\nu-1)\,-} + e^{-}\,,$$

then according to Equation 3.17 the following relation holds for the exchange current density:

$$j_0 = {}^{0}\!j \cdot \left[\mathrm{Ag}^{+}\right]^{1-\alpha} \cdot \left[\mathrm{CN}^{-}\right]^{\nu\cdot(1-\alpha)} \cdot \left[\mathrm{Ag(CN)}_{\nu}^{(\nu-1)\,-}\right]^{\alpha}\,.$$

With the Nernst relationship for the equilibrium potential ε_0 of the electrode, the dependence of the exchange current density on the cyanide concentration at a constant Ag^{+} total concentration follows as, [16]:

$$\frac{\partial \ln(j_0)}{\partial \ln\left[\mathrm{CN}^{-}\right]} = \nu + \frac{\alpha}{\Phi}\cdot\frac{\partial\varepsilon_0}{\partial \ln\left[\mathrm{CN}^{-}\right]}\,; \quad \Phi = \frac{\mathscr{R}T}{\mathscr{F}}\,.$$

With the help of this relationship we can determine the desired coordination number ν of the complex being discharged if the charge transfer coefficient α is known.

The initial current-voltage curve was determined in the same way as for zinc. A measurement at high CN^{-} concentration is shown in Figure 4.1. The curve corresponds very well to the theoretical course for a discharge reaction with the charge transfer coefficient being $\alpha = 0.5$.

To analyze the reaction mechanism, we calculated j_0 from the slope of the initial current-voltage curves at the equilibrium potential for different CN^{-} concentrations. The values obtained are plotted on a logarithmic scale against the CN^{-} concentration in Figure 4.2. The course of the curve indicates the coexistence of two different discharge steps. From the slope of the straight parts of the curve and the experimentally found relationship between equilibrium potential and CN^{-} concentration:

$$\frac{1}{\Phi}\cdot\frac{\partial\varepsilon_0}{\partial \ln\left[\mathrm{CN}^{-}\right]} = -3\,,$$

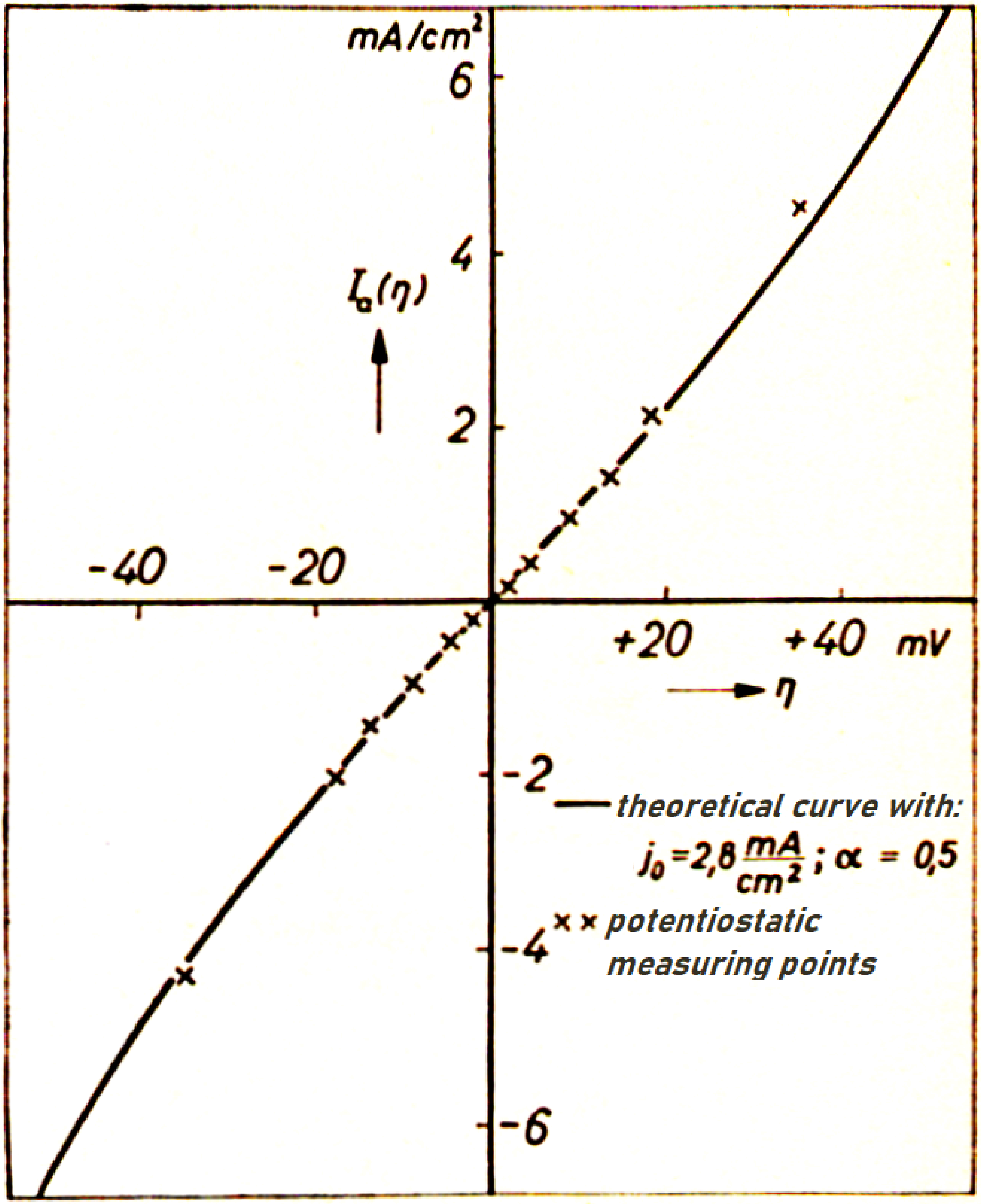

Figure 4.1.: Initial current-voltage curve of the system $Ag/[Ag(CN)_x]^{(x-1)-}$ in KCN + KCl solution at 24 °C. CN^- concentration: 1 M. Ag^+ total concentration: 2.8×10^{-2} M. Equilibrium potential: −810 mV versus n-calomel electrode

(i.e., $[\mathrm{Ag(CN)_3}]^{2-}$ is the complex predominant in solution), it follows for $\left[\mathrm{CN^-}\right] > 2 \times 10^{-1}\,\mathrm{M}$:

$$\frac{\partial j_0}{\partial \ln \left[\mathrm{CN^-}\right]} = 0.44 = \nu - 3 \cdot \alpha\,.$$

According to Figure 4.1 under these conditions $\alpha = 0.5$ and therefore $\nu = 1.94$, i.e. $\nu = 2$. *At high CN⁻ concentrations, the discharge occurs preferably via* $[Ag(CN)_2]^-$.

At a low $\mathrm{CN^-}$ concentration, the initial current-voltage curve drawn in Figure 4.3 gave the value for the charge transfer coefficient: $\alpha' = 0.44$. Under these conditions one obtains from Figure 4.2:

$$\frac{\partial \ln(j_0)}{\partial \ln \left[\mathrm{CN^-}\right]} = -0.26 = \nu' - 3 \cdot 0.44$$

$$\nu' = 1.06\,,$$

i.e. *at* $\left[CN^-\right] < 1 \times 10^{-1}\,\mathrm{M}$ *the discharge occurs preferably via* $[AgCN]$.

It is interesting to compare these results with AC measurements on the system Cd-Amalgam/$\mathrm{CN^-}$ solution, [17], where at high $\mathrm{CN^-}$ concentration ($\left[\mathrm{CN^-}\right] > 1 \times 10^{-1}\,\mathrm{M}$) the complex with a larger coordination number is also preferentially discharged. The interpretation of the curve given there undoubtedly also applies here. The competition between collision number and potential-dependent activation energy regarding the speed of ion exit favors the formation or discharge of the complex with a higher coordination number at high concentrations of the complexing agent.

4.2. Ag$^+$ Complexes with Ammonia

The initial current-voltage curves obtained in ammoniacal solution do not correspond very well to the theoretically expected course. Figure 4.4 gives an example of this[1].

The curve is too flat near the equilibrium potential. This is probably due to a contribution of the inhibition of the grows of the lattice structure or degradation at small overvoltages. If η is larger, such an inhibition of lattice incorporation should be eliminated by the formation of new crystal nuclei. This explains the increasing steepness of the current-voltage curve. Such deviations from the shape of the current-voltage curve for pure discharge can already be seen in Figure 4.3. They occurred to an increased extent in measurements in simple $\mathrm{Ag^+}$ ion solutions. A precise analysis of these findings requires further investigation.

To determine the discharge mechanism of the $[\mathrm{Ag(NH_3)_2}]^+$ ion, the method used for the cyanide complex was not applicable in this situation. We therefore used the other method, which is specifically tailored to the potentiostatic measurement method and

---

[1] The difference between the initial current densities determined by direct extrapolation and those determined by comparison with the curve for pure diffusion is probably due to the effect of the surface roughness of the solid electrode. Since the geometric surface becomes decisive for diffusion as soon as the penetration depth of the concentration wave is large compared to the roughness of the true surface, the currents at a solid electrode must decrease more strongly over time than corresponds to the requirements of the calculation in Part I. The I_a values related to the diffusion-determined current curve become smaller.

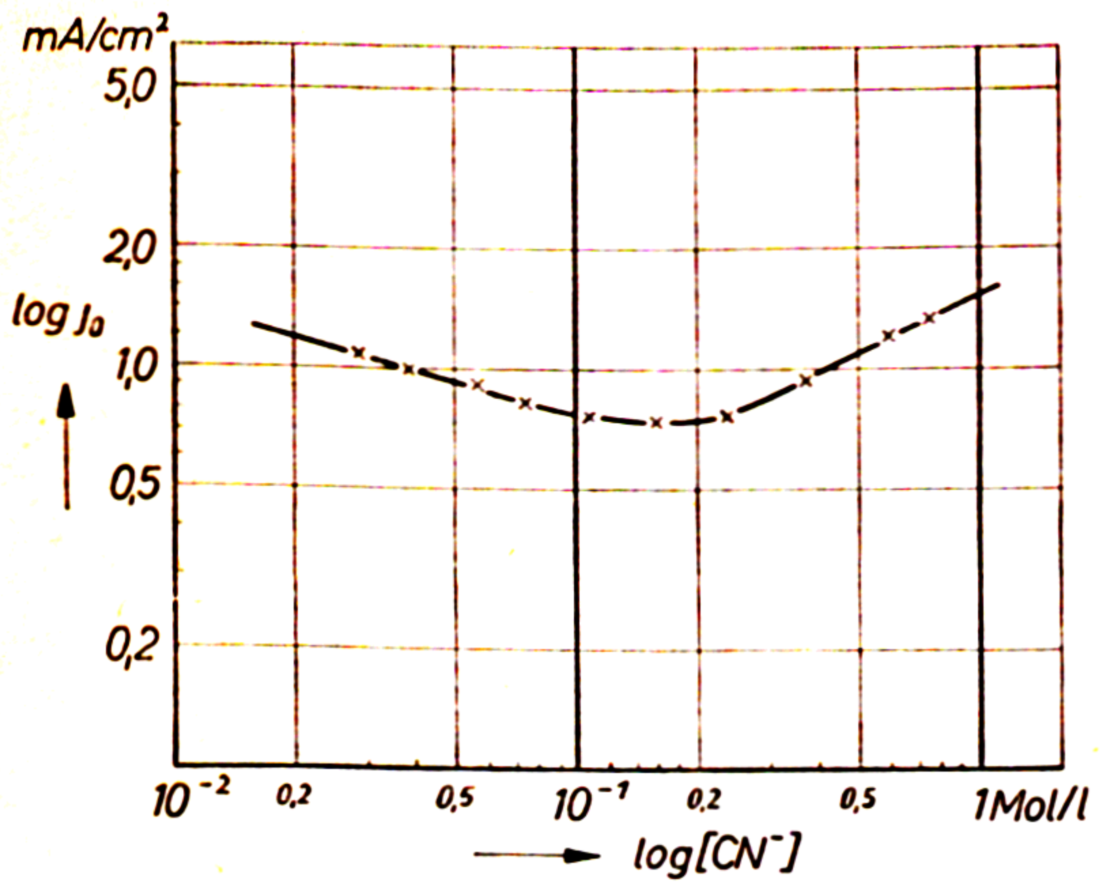

Figure 4.2.: Dependence of the exchange current density in KCN + KCl solution on the CN^- concentration at constant ionic strength and constant Ag^+ total concentration ($\left[Ag^+\right] = 5 \times 10^{-3}\,M$)

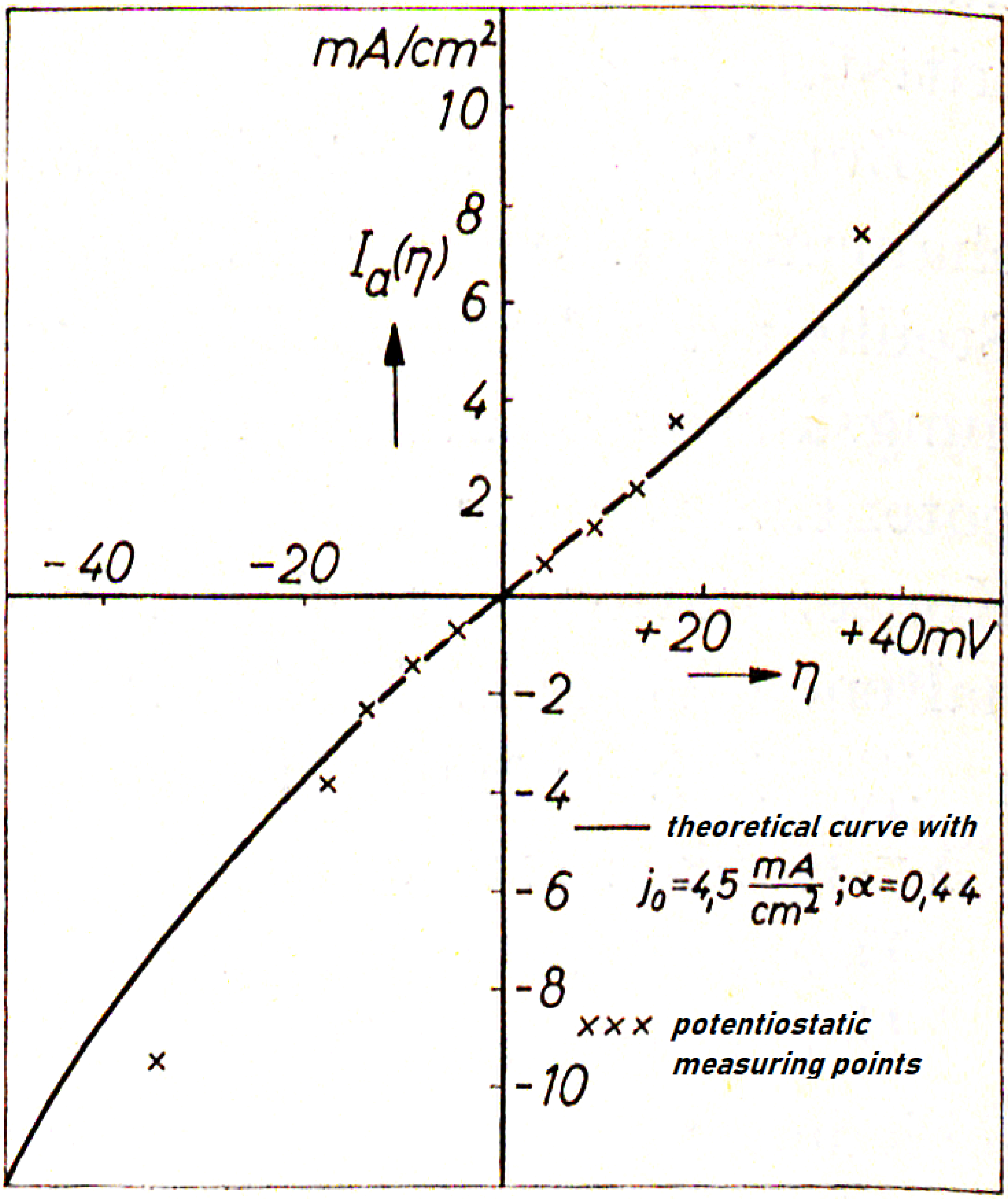

Figure 4.3.: Initial current-voltage curve at $Ag/[Ag(CN)_x]^{(x-1)-}$ in KCN + KCl solution at 24 °C. CN^- concentration: 3×10^{-2} M. Ag^+ total concentration: 1×10^{-2} M. Equilibrium potential: −628 mV versus n-calomel electrode

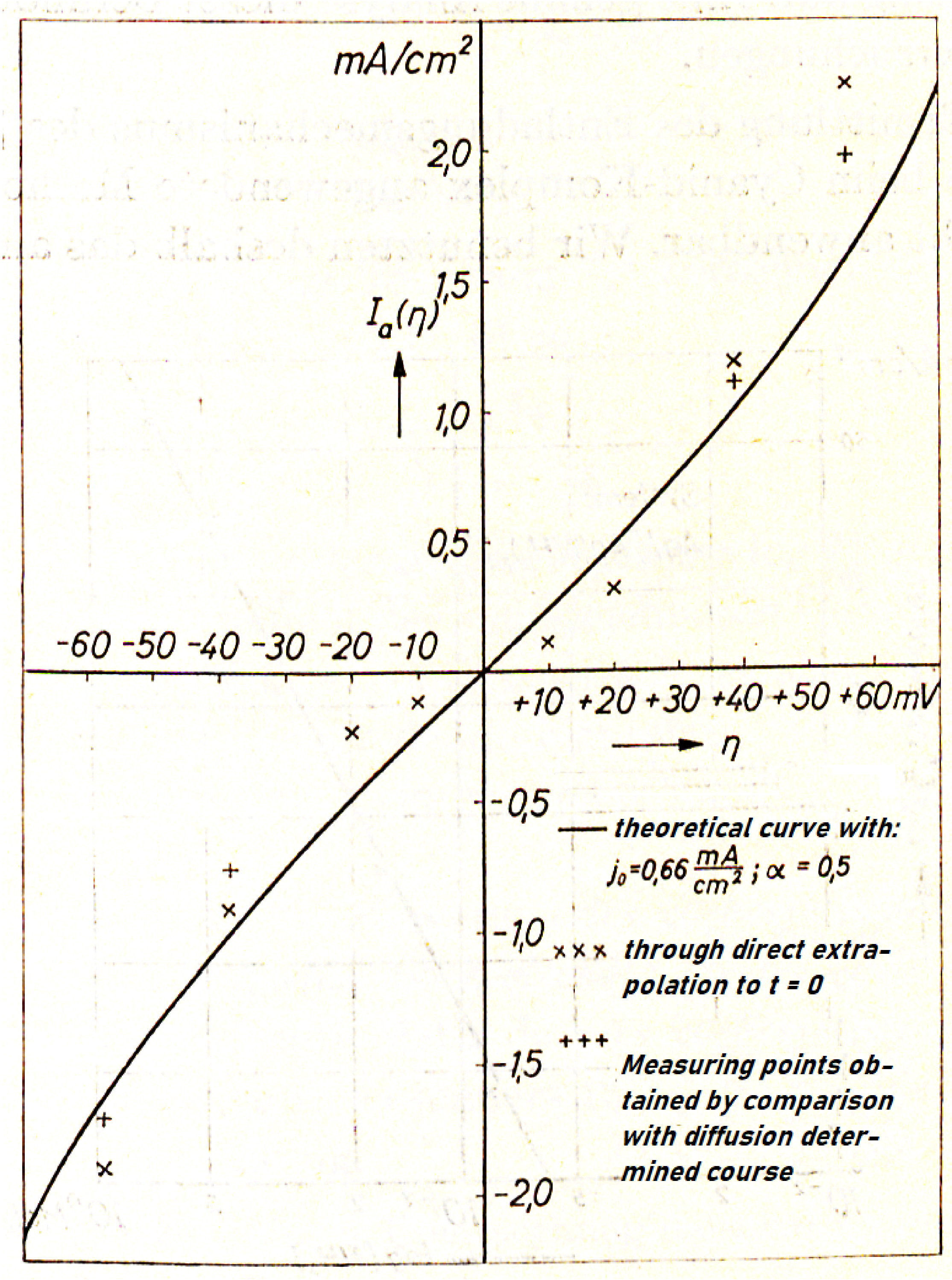

Figure 4.4.: Initial current-voltage curve at $Ag/[Ag(NH_3)_2]^+$ in NH_3 + $NaClO_4$ solution at 24 °C. NH_3 concentration: 1.8 M. Ag^+ total concentration: 2×10^{-3} M. Equilibrium potential −108 mV against n-calomel electrode

explained in Part I, which does not rely on measurements near equilibrium.
This method is based on comparing the anodic partial current of the pure discharge at the same electrode potential while varying the concentration of the complexing agent. In this specific case, the following applies to the charge transfer current according to Equation 4.2:

$$\begin{aligned} j &= k^+\,[\mathrm{Ag}]\cdot[\mathrm{NH_3}]^{\nu}\cdot e^{\frac{\alpha}{\Phi}\cdot\varepsilon} - k^-\left[\mathrm{Ag(NH_3)}_{\nu}^{+}\right]\cdot e^{-\frac{(1-\alpha)}{\Phi}\cdot\varepsilon} \\ &= I_a^+ \qquad\qquad\qquad\qquad\qquad - I_a^- \,. \end{aligned}$$

With constant ε there results:
according to Equation 4.3

$$I_a^+ \sim [\mathrm{NH_3}]^{\nu}$$

and according to Equation 4.4

$$\frac{\partial \log(I_a^+)}{\partial \log\,[\mathrm{NH_3}]} = \nu\,.$$

The anodic initial partial current I_a^+ is calculated from the measured current density I_a according to Equation 3.3 as:

$$I_a^+ = \frac{I_a}{1 - e^{-\frac{(\varepsilon-\varepsilon_0)}{\Phi}}}\,. \tag{4.6}$$

In Figure 4.5 $\log(I_a^+)$ is plotted against $\log\,[\mathrm{NH_3}]$ from such a series of measurements. From the steepness of the drawn line it follows that $\nu = 2$. In the concentration range under consideration, $[\mathrm{Ag(NH_3)_2}]^+$ is the preferred complex for discharge.
The discharge of $\mathrm{Ag}^+_{\mathrm{aq}}$ ions plays practically no role here either.
In this case, the discharge of the predominant complex occurs directly without prior decay into intermediate products. The method used to clarify this reaction is particularly recommended for all processes with not too small discharge inhibition due to its easy evaluation.

We would like to thank Prof. K. F. Bonhoeffer for his support of this research.

From the Max-Planck-Institute for physical chemistry in Göttingen.

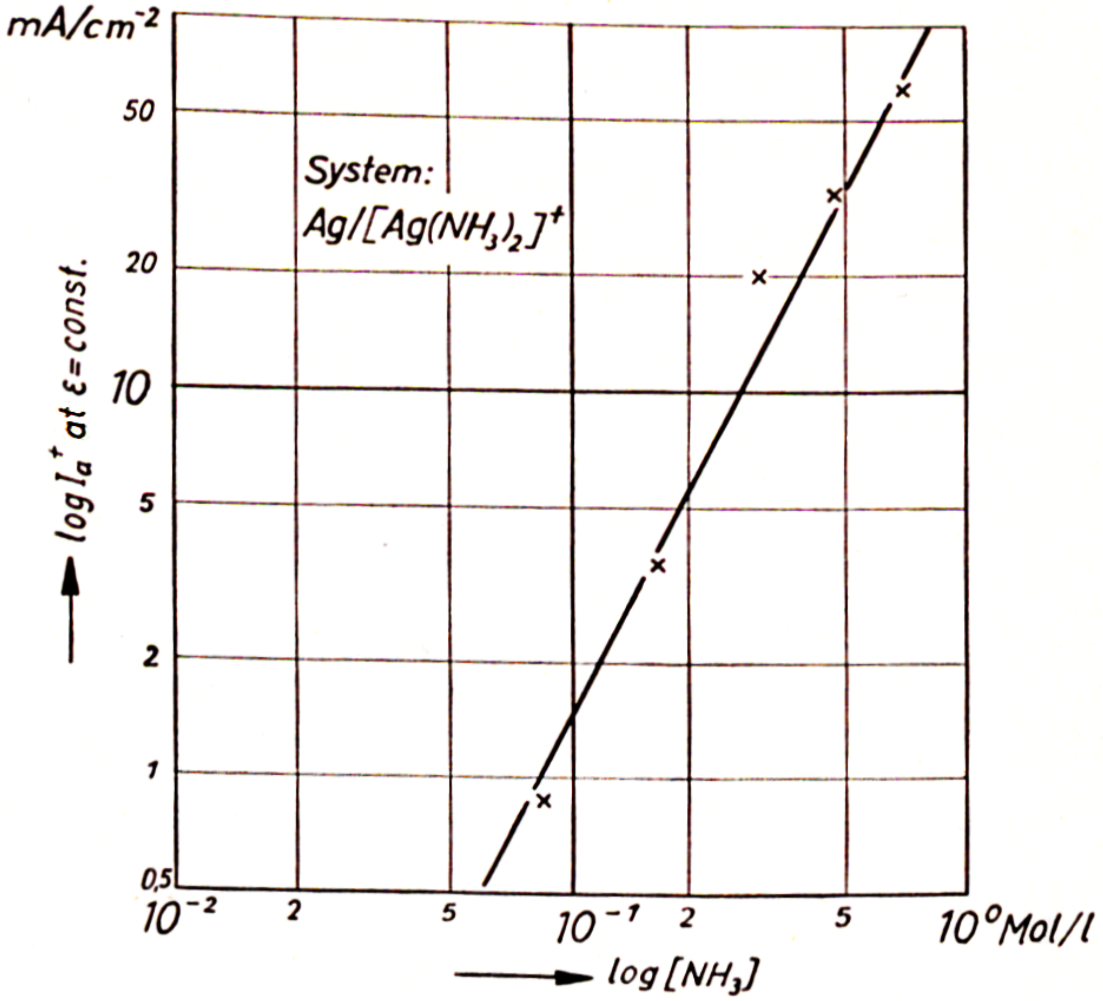

Figure 4.5.: Dependence of the anodic initial partial current on the NH_3 concentration at constant potential: $\varepsilon = +165\,\mathrm{mV}$ versus n-calomel electrode. Temperature: 24 °C. Ag^+ total concentration: $1 \times 10^{-2}\,\mathrm{M}$

Part III.

Appendix

1. Calculation of the concentration curve over time

We have to solve the differential equation system Equation 3.6 with the boundary conditions Equation 3.7a to Equation 3.7c where we use the LAPLACE transformation, [9]. We rewrite the boundary condition Equation 3.7c with Equation 3.2 in the form:

$$\left.\begin{aligned} \left(\frac{\partial c_{0x}}{\partial x}\right)_{x=0} &= \lambda_{0x} \cdot c_{0x} - \varkappa \cdot \lambda_r \cdot c_r \\ \left(\frac{\partial c_r}{\partial x}\right)_{x=0} &= \frac{\lambda_{0x}}{\varkappa} \cdot c_{0x} - \lambda_r \cdot c_r \end{aligned}\right\} \tag{1.1}$$

with

$$\left.\begin{aligned} \lambda_{0x} &= \frac{j_0 \cdot e^{-(1-\alpha)\cdot\frac{n}{\varphi}\cdot\eta}}{n \cdot \mathscr{F} \cdot \mathscr{D}_{0x} \cdot {}_0c_{0x}} \\ \lambda_r &= \frac{j_0 \cdot e^{\alpha\cdot\frac{n}{\varphi}\cdot\eta}}{n \cdot \mathscr{F} \cdot \mathscr{D}_r \cdot {}_0c_r} \\ \varkappa &= \frac{\mathscr{D}_r}{\mathscr{D}_{0x}}\,. \end{aligned}\right\} \tag{1.2}$$

The LAPLACE transformation is:

$$\left.\begin{aligned} f(s,x) = L\left\{c_{0x}(t,x)\right\} &= \int_0^\infty e^{-s\cdot t} \cdot c_{0x}(t,x)\,\mathrm{d}t \\ g(s,x) = L\left\{c_r(t,x)\right\} &= \int_0^\infty e^{-s\cdot t} \cdot c_r(t,x)\,\mathrm{d}t\,. \end{aligned}\right\} \tag{1.3}$$

Transformation of the differential equation Equation 3.6 gives the ordinary differential equations with Equation 3.7a:

$$\left.\begin{aligned} s \cdot f(s,x) - {}_0c_{0x} &= \mathscr{D}_{0x} \cdot \frac{\partial^2 f(s,x)}{\partial x^2} \\ s \cdot g(s,x) - {}_0c_r &= \mathscr{D}_r \cdot \frac{\partial^2 g(s,x)}{\partial x^2} \end{aligned}\right\} \tag{1.4}$$

The transformation of the boundary conditions in Equation 3.7a and Equation 3.7c provides two further pairs of equations:

$$\left.\begin{aligned} f(s, x=\infty) &= \frac{{}_0c_{0x}}{s} \\ g(s, x=-\infty) &= \frac{{}_0c_r}{s}\,, \end{aligned}\right\} \tag{1.5}$$

$$\left.\begin{aligned}\left(\frac{\partial f(s,x)}{\partial x}\right)_{x=0} &= \lambda_{0x}\cdot f(s,0) - \varkappa\cdot\lambda_r\cdot g(s,0)\\ \left(\frac{\partial g(s,x)}{\partial x}\right)_{x=0} &= \frac{\lambda_{0x}}{\varkappa}\cdot f(s,0) - \lambda_r\cdot g(s,0)\,.\end{aligned}\right\} \tag{1.6}$$

The solution of Equation 1.4 reads: (taking into account Equation 1.5)

$$\left.\begin{aligned}f(s,x) &= \alpha(s)\cdot e^{-\sqrt{\frac{s}{\mathscr{D}_{0x}}}\cdot x} + \frac{{}_0c_{0x}}{s}\\ g(s,x) &= \beta(s)\cdot e^{+\sqrt{\frac{s}{\mathscr{D}_{r}}}\cdot x} + \frac{{}_0c_{r}}{s}\,.\end{aligned}\right\} \tag{1.7}$$

$\alpha(s)$ and $\beta(s)$ can be calculated from Equation 1.7 with the help of Equation 1.6. Hence:

$$\alpha(s) = \frac{A}{s\cdot(\lambda+\sqrt{s})} = -\sqrt{\varkappa}\cdot\beta(s) \tag{1.8}$$

with:

$$\left.\begin{aligned}A &= \sqrt{\mathscr{D}_r}\cdot\lambda_r\cdot{}_0c_r - \sqrt{\mathscr{D}_{0x}}\cdot\lambda_{0x}\cdot{}_0c_{0x}\\ \lambda &= \sqrt{\mathscr{D}_r}\cdot\lambda_r + \sqrt{\mathscr{D}_{0x}}\cdot\lambda_{0x}\,.\end{aligned}\right\} \tag{1.9}$$

We are only interested in the solution at the electrode, i.e. for $x = 0$. The inverse transformation of Equation 1.7 and Equation 1.8 yields according to Doetsch, [9]:

$$\left.\begin{aligned}c_{0x}(t,0) &= {}_0c_{0x} + \frac{A}{\lambda}\cdot\left(1 - e^{\lambda^2\cdot t}\cdot\operatorname{erfc}\left(\lambda\sqrt{t}\right)\right)\\ c_r(t,0) &= {}_0c_r - \frac{\sqrt{\varkappa}\cdot A}{\lambda}\cdot\left(1 - e^{\lambda^2\cdot t}\cdot\operatorname{erfc}\left(\lambda\sqrt{t}\right)\right)\,.\end{aligned}\right\} \tag{1.10}$$

After inserting these relationships into Equation 3.2, finally for the current we get Equation 3.8.

Bibliography

[1] H. W. Bode. *Network Analysis and Feedback Amplifier design.* The Bell Telephone Laboratories Series. D. Van Nostrand Company, Inc., Princeton, New Jersey, Toronto, London, New York, 1 edition, 1945.

[2] J. A. V. Butler. Studies in heterogeneous equilibria. Part III. A kinetic theory of reversible oxidation potentials at inert electrodes. *Transactions of the Faraday Society*, 19:734–739, 1924.

[3] J. A. V. Butler. The mechanism of overvoltage and its relation to the combination of hydrogen atoms at metal electrodes. *Transactions of the Faraday Society*, 28:379–382, 1932.

[4] J. A. V. Butler. *Electrical Phenomena at Interphases.* Methuen a. Co., London, 1 edition, 1951.

[5] F. G. Cottrell. Der Reststrom bei galvanischer Polarisation, betrachtet als ein Diffusionsproblem. *Zeitschrift für physikalische Chemie*, 42(4):385–431, 1903.

[6] P. Delahay. Theory of Polarographic Currents Controlled by Rate of Reaction and by Diffusion. *Journal of the American Chemical Society*, 73(10):4944–4949, 1951.

[7] P. Delahay. Unified Theory of Polarographic Waves. *Journal of the American Chemical Society*, 75(6):1430–1435, 1953.

[8] P. Delahay and T. Berzins. Theory of Electrolysis at Constant Current with Partial or Total Control by Diffusion-Application to the Study of Complex Ions. *Journal of the American Chemical Society*, 75(10):2486–2493, 1953.

[9] G. Doetsch. *Tabellen zur* LAPLACE-*Transformation und Anleitung zum Gebrauch*, volume LIV of *Die Grundlehren der mathematischen Wissenschaften in Einzeldarstellungen.* Springer-Verlag Berlin und Göttingen, 1 edition, 1947.

[10] B. V. Ershler. *Zhurnal Fizicheskoi Khimii (U.S.S.R.)*, 22:683, 1948.

[11] B. V. Ershler. *Zhurnal Fizicheskoi Khimii (U.S.S.R.)*, 22:1344, 1948.

[12] H. Gerischer. Die Austauschstromdichte beim Gleichgewichtspotential an Elektroden mit einem potentialbestimmenden Vorgang. *Zeitschrift für Elektrochemie und angewandte physikalische Chemie*, 54(5):362–365, 1950.

[13] H. Gerischer. Bestimmung der Austauschgeschwindigkeit beim Gleichgewichtspotential durch Polarisationsmessungen mit Gleich- und Wechselstrom. *Zeitschrift für Elektrochemie und angewandte physikalische Chemie*, 55(2):98–104, 1951.

[14] H. Gerischer. Wechselstrompolarisation von Elektroden mit einem potentialbestimmenden Schritt beim Gleichgewichtspotential I. *Zeitschrift für physikalische Chemie*, 198(5-6):286–313, 1951.

[15] H. Gerischer. Kinetik der Entladung einfacher und komplexer Zink-Ionen. *Zeitschrift für physikalische Chemie*, 202(3-4):302–317, 1953.

[16] H. Gerischer. Uber die kinetische Analyse des Entladungsmeclianismus von Komplex-Ionen. *Zeitschrift für physikalische Chemie*, 202:292–301, 1953.

[17] H. Gerischer. Zum Entladungsmechanismus von Komplex-Ionen. *Zeitschrift für Elektrochemie und angewandte physikalische Chemie*, 57(7):604–609, 1953.

[18] H. Gerischer and R. P. Tischer. Isotopenaustausch und Umlagerungsvorgänge in Silberoberflächen. *Zeitschrift für Elektrochemie und angewandte physikalische Chemie*, 58(10):819–827, 1954.

[19] H. Gerischer and K. J. Vetter. Konzentrationspolarisation bei vorgelagerter chemischer Reaktion im Elektrolyten und ihr Anteil am stationären Polarisationswiderstand beim Gleichgewichtspotential. *Zeitschrift für Physikalische Chemie*, 197(1-2):92–104, 1951.

[20] L. Gierst and A. Juliard. Non-steady State Electrolysis under Constant Forced Current. *Journal of Physical Chemistry*, 57(7):701–706, 1953.

[21] K.-H. Henke and W. Hans. Zur Theorie der polarographischen Kurve VI Reaktionskinetisch bedingte polarographische Stromstärke: 1. Mitteilung: Theoretischer Teil. *Zeitschrift für Elektrochemie und angewandte physikalische Chemie*, 57(7):591–595, 1953.

[22] A. L. Hodgkin, A. F. Huxley, and B. Katz. Ionic currents underlying activity in the giant axon on the squid. *Archives des Sciences Physiologiques*, 3:129–150, 1949.

[23] N. Ibl and G. Trümpler. Über zwei Elektrolyseprobleme mit linearer Diffusion bei Abwesenheit von Konvektionen. *Helvetica Chimica Acta*, 34(5):1217–1223, 1951.

[24] E. Jahnke and F. Emde. *Tafeln höherer Funktionen.* B. G. Teubner, Leipzig, 4 edition, 1948.

[25] J. Koutecky and R. Brdicka. Fundamental equation for the electrolytic current when depending on the formation rate of the depolariser jointly with diffusion and its polarographic verification. *Collection of Czechoslovak Chemical Communications*, 12:337–355, 1947.

[26] H. A. Laitinen and I. M. Kolthoff. A Study of Diffusion Processes by Electrolysis with Microelectrodes. *Journal of the American Chemical Society*, 61(12):3344–3349, 1939.

[27] J. J. Lingane. *Electroanalytical Chemistry.* Interscience Publ. Inc., New York und London, 1 edition, 1953.

[28] J. E. B. Randles. Kinetics of rapid electrode reactions. *Discussions of the Faraday Society*, 1:11–19, 1947.

[29] J. Schoen and K. E. Staubach. Ein elektronischer Potentiostat mit kleiner Einstellzeit. *Regelungstechnik*, 2(7):157–162, 1954.

[30] M. Smutek. Number III in Proceedings of the 1. International Polorographic Congress in Prague, page 687, 1951.

[31] M. V. Stackelberg, M. Pilgram, and V. Toome. Bestimmung von Diffusionskoeffizienten einiger Ionen in wäßriger Lösung in Gegenwart von Fremdelektrolyten. I. *Zeitschrift für Elektrochemie und angewandte physikalische Chemie*, 57(5):342–350, 1953.

[32] F. E. Terman. *Radio Engineers Handbook*. McGraw-Hill Electrical and Electronic Engineering Series. McGraw-Hill Book Company, Inc., New York and London, 1 edition, 1943.